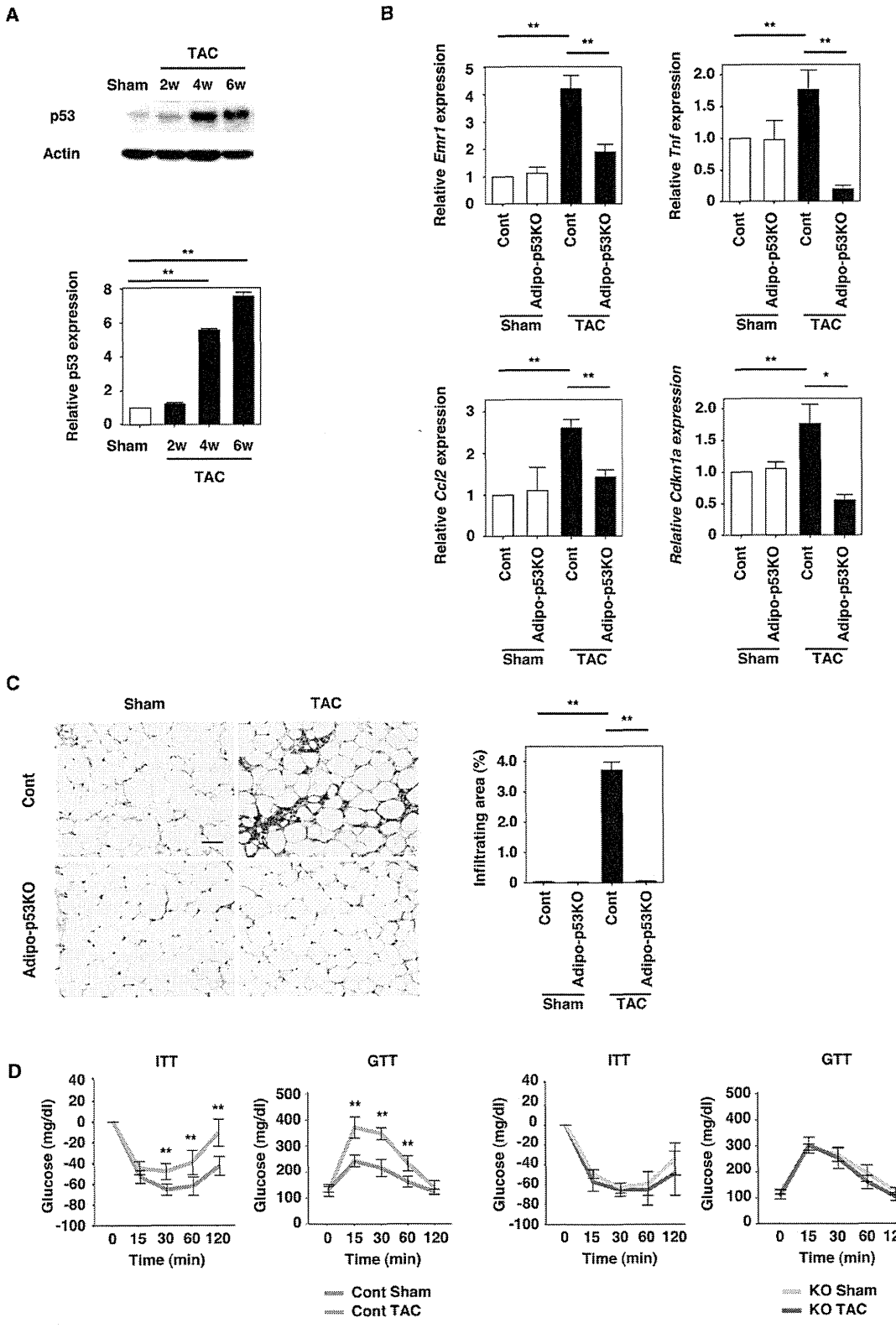
A
TAC
Sham 2w 4w 6w
p53
Actin
Relative p53 expression
Sham 2w 4w 6w
TAC
B
Relative Emr1 expression
Relative Tnf expression
Relative Ccl2 expression
Relative Cdkn1a expression
Cont
Adipo-p53KO
Sham
TAC
C
Sham
TAC
Cont
Adipo-p53KO
Infiltrating area (%)
D
ITT
GTT
Glucose (mg/dl)
Time (min)
Cont Sham
Cont TAC
KO Sham
KO TAC

(Figures 2B and 2C). Consequently, adipo-p53 KO mice showed improved insulin sensitivity and glucose tolerance after induction of pressure overload compared with littermate controls (Figure 2D) without any change of food intake (Figure S2C). These results suggest that p53 has a critical role in the regulation of adipose tissue inflammation and insulin resistance during pressure overload. In contrast, a decrease of fat mass and an increase of plasma free fatty acids were observed to a similar extent in both adipo-p53 KO and control mice after TAC (Figures S2D–S2F), suggesting that pressure overload accelerates lipolysis in a p53-independent manner.

Pressure Overload Promotes Lipolysis via the Sympathetic Nervous System

We inhibited sympathetic activity in epididymal fat tissue by surgical denervation and then performed TAC. As a result, surgical denervation effectively inhibited an increase of the norepinephrine level of adipose tissue and attenuated lipolysis after the onset of pressure overload (Figures S3A and S3B and data not shown). Histological examination of adipose tissue showed that infiltration of inflammatory cells after TAC was attenuated by denervation (Figures S3C and S3D). Likewise, disruption of the sympathetic efferent nerves significantly reduced pressure overload-induced upregulation of *Emr1*, a proinflammatory cytokine expression in adipose tissue (Figure 3A), and this reduction was associated with significant improvement of insulin resistance and glucose tolerance in TAC mice (Figure 3B). Surgical denervation attenuated pressure overload-induced upregulation of p53 and *Cdkn1a* expression in adipose tissue (Figures 3A and 3C). We also pharmacologically inhibited the sympathetic activity in adipose tissue by injecting guanethidine directly into epididymal fat and then performed TAC. As a result, pharmacological denervation also significantly inhibited lipolysis (Figures S3A and S3B) and attenuated upregulation of p53 and *Cdkn1a* expression and inflammation in adipose tissues (Figures S3C, S3D, S4A and S4B). Mice treated with guanethidine showed better insulin sensitivity and glucose tolerance after creation of pressure overload (Figure S4C), indicating that pressure overload-induced activation of the sympathetic nervous system accelerates lipolysis and, thus, leads to adipose tissue inflammation and insulin resistance in TAC mice.

Role of Lipolysis in the Regulation of Adipose p53 Expression and Inflammation

To examine the role of lipolysis in influencing adipose tissue expression of p53 and inflammation after TAC, we inhibited lipolysis by administering acipimox, a selective inhibitor of lipolysis, to mice with TAC. Treatment with acipimox markedly inhibited lipolysis and also reduced infiltration of inflammatory cells into adipose tissue during pressure overload (Figures S3A–S3D). Inhibition of lipolysis also significantly reduced pressure overload-induced upregulation of *Emr1* and proinflammatory cytokine production in adipose tissue (Figure 4A), along with significant improvement of insulin resistance and glucose intolerance in TAC mice (Figure 4B). Furthermore, treatment with acipimox attenuated pressure overload-induced upregulation of p53 and *Cdkn1a* expression in adipose tissue (Figures 4A and 4C), confirming a close relationship between lipolysis and p53 expression.

Next, we promoted lipolysis by administering isoproterenol to mice via an infusion pump. Treatment with isoproterenol significantly decreased the visceral fat mass and increased plasma fatty acid levels (Figures S5A–S5C) and increased p53 expression in adipose tissue (Figure 5A). Isoproterenol also induced adipose tissue inflammation (Figures 5B and 5C). To further investigate the role of lipolysis in the regulation of p53 expression and inflammation in adipose tissue, we tested the influence of deleting adipose triglyceride lipase (patatin-like phospholipase domain containing protein 2, encoded by *Pnpla2*; hereafter referred to as Atgl) on adipose tissue expression of p53. It has been reported that Atgl homozygous KO mice show massive accumulation of lipids in the heart, causing cardiac dysfunction and premature death (Haemmerle et al., 2006). When we generated TAC mice, we also noted that cardiac function was worse and LV enlargement was more marked in Atgl heterozygous KO mice compared with their littermates (Figure S5D). In fact, most of the KO mice died of heart failure within 4 weeks after TAC. Therefore, we utilized Atgl-deficient adipose tissue for ex vivo experiments. We cultured epididymal fat pad tissues from Atgl KO mice or wild-type littermates and examined the effect of isoproterenol on p53 expression. Treatment of wild-type fat pads with isoproterenol significantly induced lipolysis (Figure 5D) and upregulated the expression of both p53 and *Cdkn1a* expression (Figures 5E and 5F). Disruption of Atgl inhibited isoproterenol-induced lipolysis (Figure 5D) and prevented the upregulation of adipose p53 and *Cdkn1a* expression (Figures 5E and 5F), suggesting a crucial role of lipolysis in the regulation of p53 expression and inflammation in adipose tissue.

Myocardial Infarction Induces Adipose Tissue Inflammation and Insulin Resistance

To investigate whether myocardial infarction (MI) induced insulin resistance, we created MI in 11-week-old mice and assessed the animals 6 weeks after surgery. Insulin sensitivity and glucose tolerance were significantly impaired in MI mice compared with sham-operated mice (Figure S5E). Significant loss of fat tissue was also observed in MI mice (Figures S5F and S5G) and this was associated with upregulation of adipose

Figure 2. p53-Dependent Adipose Tissue Inflammation Provokes Systemic Insulin Resistance during Heart Failure

(A) Expression of p53 was examined in adipose tissues of mice by western blot analysis at indicated time points after sham operation (Sham) or TAC. Actin was used as an equal loading control. The graph indicates the quantitative data on p53 expression (n = 3).

(B) Real-time PCR assessing the expression of *Emr1*, *Tnf* (Tnfα), *Ccl2* (MCP1), and *Cdkn1a* (p21) levels in adipose tissue of adipocyte-specific p53-deficient mice (adipo-p53 KO) and littermate controls (Cont) at 6 weeks after sham operation or TAC procedure (n = 12).

(C) Hematoxylin and eosin staining of adipose tissues of adipocyte-specific p53-deficient mice (adipo-p53 KO) and littermate controls (Cont) at 6 weeks after sham operation (Sham) or TAC procedure. Scale bar, 50 μm. The right graph indicates the quantitative data on the infiltration of macrophages (n = 4).

(D) Insulin tolerance test (ITT) and glucose tolerance test (GTT) in adipocyte-specific p53-deficient mice (KO) and littermate controls (Cont) at 6 weeks after sham operation (Sham) or TAC procedure (n = 16). Data are shown as the means ± S.E.M. *$p < 0.05$, **$p < 0.01$.

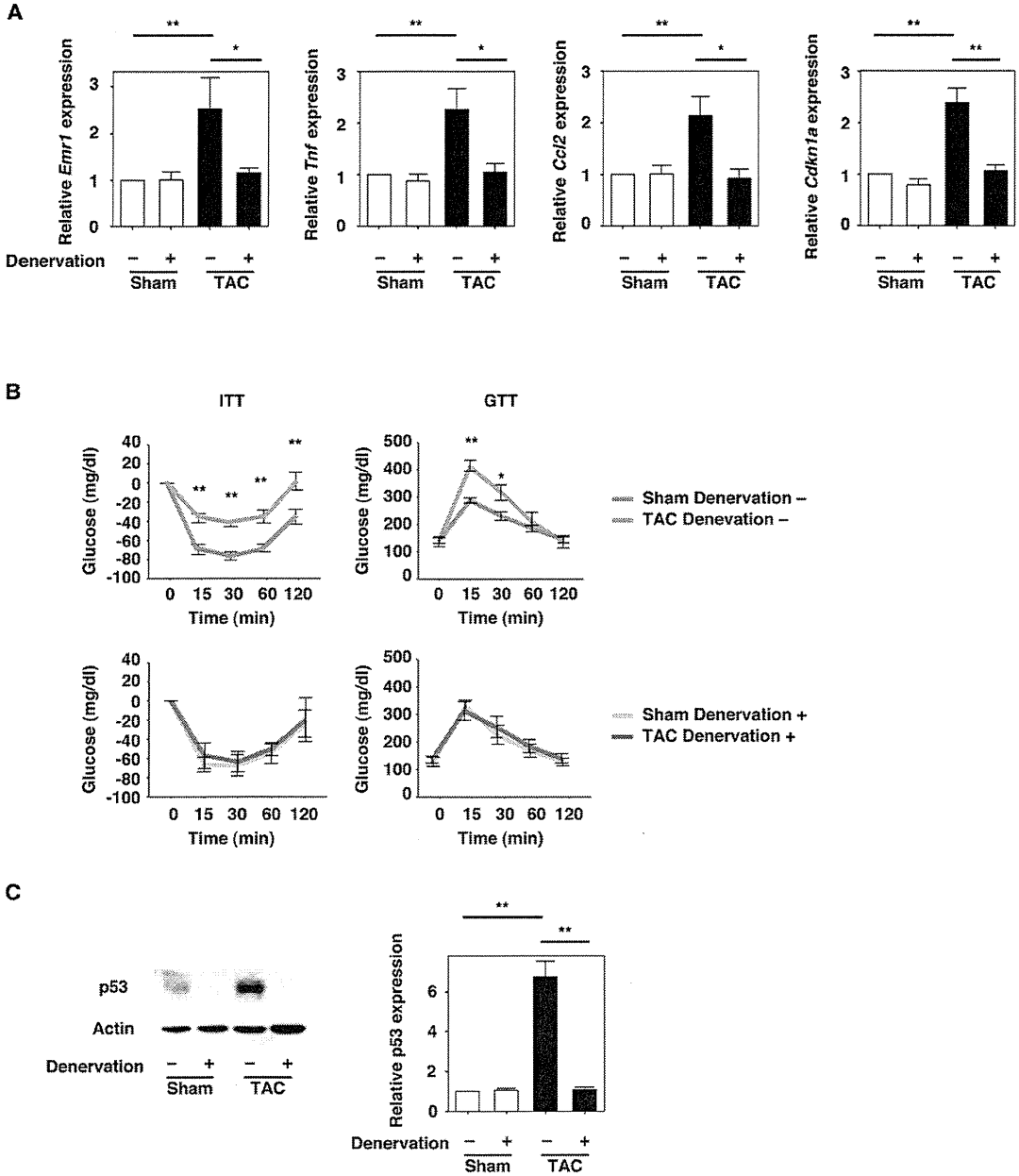

Figure 3. Surgical Transection of the Sympathetic Nerves Attenuates Adipose Tissue Inflammation and Systemic Insulin Resistance

(A) Real-time PCR assessing the expression of *Emr1*, *Tnf* (Tnfα), *Ccl2* (MCP1), and *Cdkn1a* (p21) levels in adipose tissues of mice at 6 weeks after sham operation (Sham) or TAC with or without surgical transection of the sympathetic nerves (Denervation) of epididymal fat (n = 8).

(B) Insulin tolerance test (ITT) and glucose tolerance test (GTT) of mice at 6 weeks after sham operation (Sham) or TAC with or without surgical denervation (n = 20).

(C) Western blot analysis of p53 in adipose tissues of mice at 6 weeks after sham operation (Sham) or TAC with or without surgical denervation. The right graph indicates the quantitative data on p53 expression (n = 3). Data are shown as the means ± S.E.M. *p < 0.05, **p < 0.01.

tissue p53 expression and inflammation (Figures S5H–S5J). Inhibition of p53 activation in adipose tissue by genetic disruption significantly attenuated inflammation of this tissue and improved metabolic abnormalities (Figures S5K and S5L). These results suggest that the same mechanism underlies insulin resistance associated with heart failure due to both pressure overload and MI.

Influence of Inhibiting p53-Induced Adipose Tissue Inflammation on Cardiac Function

To investigate whether inhibition of p53-induced adipose tissue inflammation could influence cardiac function in the development of heart failure, we performed TAC and monitored cardiac function in adipo-p53 KO mice. We found that adipo-p53 KO mice showed significantly better cardiac function and less LV

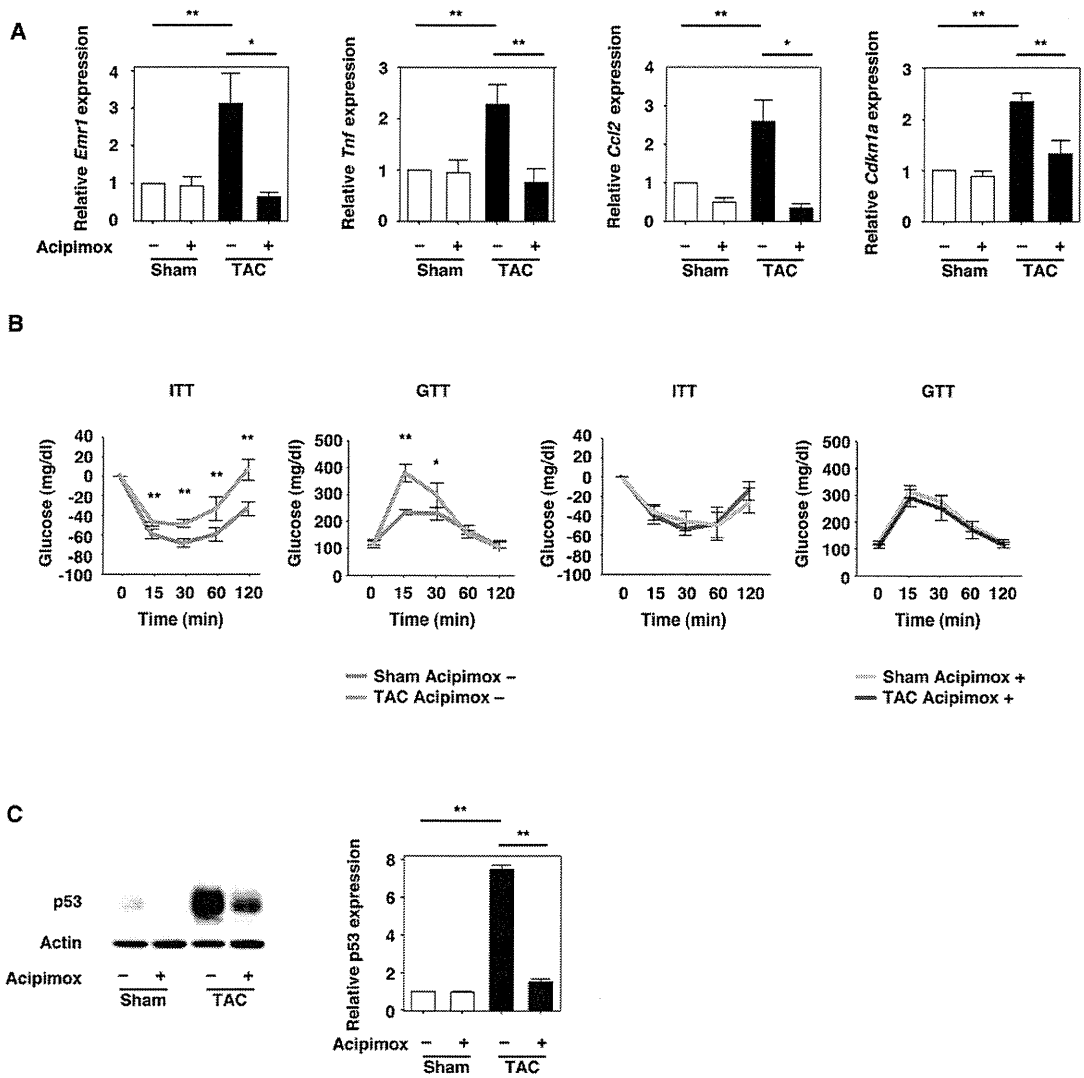

Figure 4. Treatment with a Lipolysis Inhibitor Ameliorates Adipose Tissue Inflammation and Systemic Insulin Resistance

(A) Real-time PCR assessing the expression of *Emr1*, *Tnf* (Tnfα), *Ccl2* (MCP1), and *Cdkn1a* (p21) levels in adipose tissue of mice at 6 weeks after sham operation (Sham) or TAC with or without acipimox treatment (n = 8).

(B) Insulin tolerance test (ITT) and glucose tolerance test (GTT) of mice at 6 weeks after sham operation (Sham) or TAC with or without acipimox treatment (n = 32).

(C) Western blot analysis of p53 in adipose tissues of mice at 6 weeks after sham operation (Sham) or TAC with or without acipimox treatment. Actin was used as an equal loading control. The right graph indicates the quantitative data on p53 expression (n = 3). Data are shown as the means ± S.E.M. *$p < 0.05$, **$p < 0.01$.

enlargement compared with their littermate controls (Figure 6A). They also showed better survival during the chronic phase of heart failure (Figure 6B). Similar results were observed in another model of heart failure induced by MI (Figure S6A). Furthermore, administration of a p53 inhibitor (pifithrin-α) into the adipose tissue of the TAC or MI model mice after the onset of heart failure improved cardiac dysfunction, as well as adipose tissue inflammation, and metabolic abnormalities (Figures 6C–6E and S6B–S6D), indicating that inhibition of p53 may be useful for the treatment of heart failure and its associated metabolic abnormalities. Moreover, we noted significant improvement of cardiac function after sympathetic nerve blockade (Figures S6E and S6F). However, treatment of TAC mice with acipimox was found to exacerbate cardiac dysfunction (Figure S6G), presumably because it impaired fatty acid metabolism and energy production in cardiomyocytes, as reported previously (Tuunanen et al., 2006).

Mechanism of p53-Induced Adipose Tissue Inflammation during Heart Failure

Because our results indicated that adrenergic activation induced lipolysis that upregulated p53 and promoted adipose tissue inflammation, we speculated that an excess of fatty acids might be involved in the upregulation of p53 in adipose tissue. Therefore, we examined the effect of palmitic acid on cultured preadipocytes. Treatment with palmitic acid significantly increased the

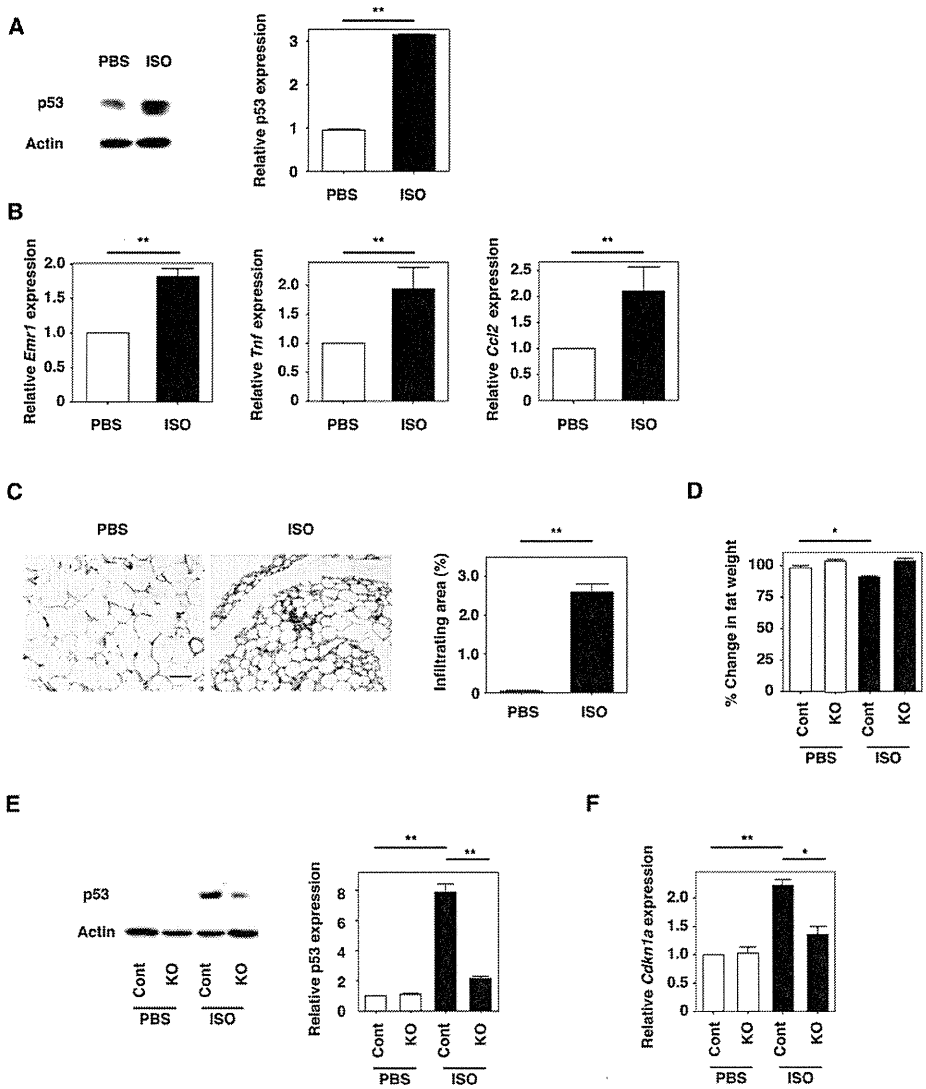

Figure 5. Role of Lipolysis in the Regulation of Adipose p53 Expression and Inflammation

(A) Western blot analysis of p53 in adipose tissues of wild-type mice treated with PBS or isoproterenol (ISO). Actin was used as an equal loading control. The right graph indicates the quantitative data on p53 expression (n = 3).

(B) Real-time PCR assessing the expression of *Emr1*, *Tnf* (Tnfα), and *Ccl2* (MCP1) levels in adipose tissues of wild-type mice treated with PBS or isoproterenol (ISO) (n = 8).

(C) Hematoxylin and eosin staining of adipose tissues of wild-type mice treated with PBS or isoproterenol (ISO). Scale bar, 50 μm. The right graph indicates the quantitative data on macrophage infiltration (n = 4).

(D) The changes in weight of adipose tissues isolated from Atgl-deficient mice (KO) and littermate controls (Cont) after treatment with PBS or isoproterenol (ISO) (n = 6).

(E) Expression of p53 was examined in adipose tissues of Atgl-deficient mice (KO) and littermate controls (Cont) treated with PBS or isoproterenol (ISO) by western blot analysis. The right graph indicates the quantitative data on p53 expression (n = 3).

(F) Real-time PCR assessing the expression of *Cdkn1a* (p21) level in adipose tissues isolated from Atgl-deficient mice (KO) and littermate controls (Cont) after treatment with PBS or isoproterenol (ISO) (n = 6). Data are shown as the means ± S.E.M. *p < 0.05, **p < 0.01.

intracellular level of reactive oxygen species (ROS) and caused DNA damage, as demonstrated by the increase of γH2AX, which in turn upregulated p53 expression (Figures 7A–7C, S7A, and S7B). This upregulation of p53 was associated with an increase of NF-κB activity and proinflammatory cytokine expression (Figures 7D and 7E). Because it has been reported that p53 enhances the activity of NF-κB, which regulates various cytokines including *TNF-α* and *CCL2* (Benoit et al., 2006; Ryan et al., 2000), we examined the relationship between p53 expression and NF-κB activation. We demonstrated that the disruption of p53 expression significantly attenuated palmitic acid-induced activation of NF-κB and upregulation of *Ccl2*

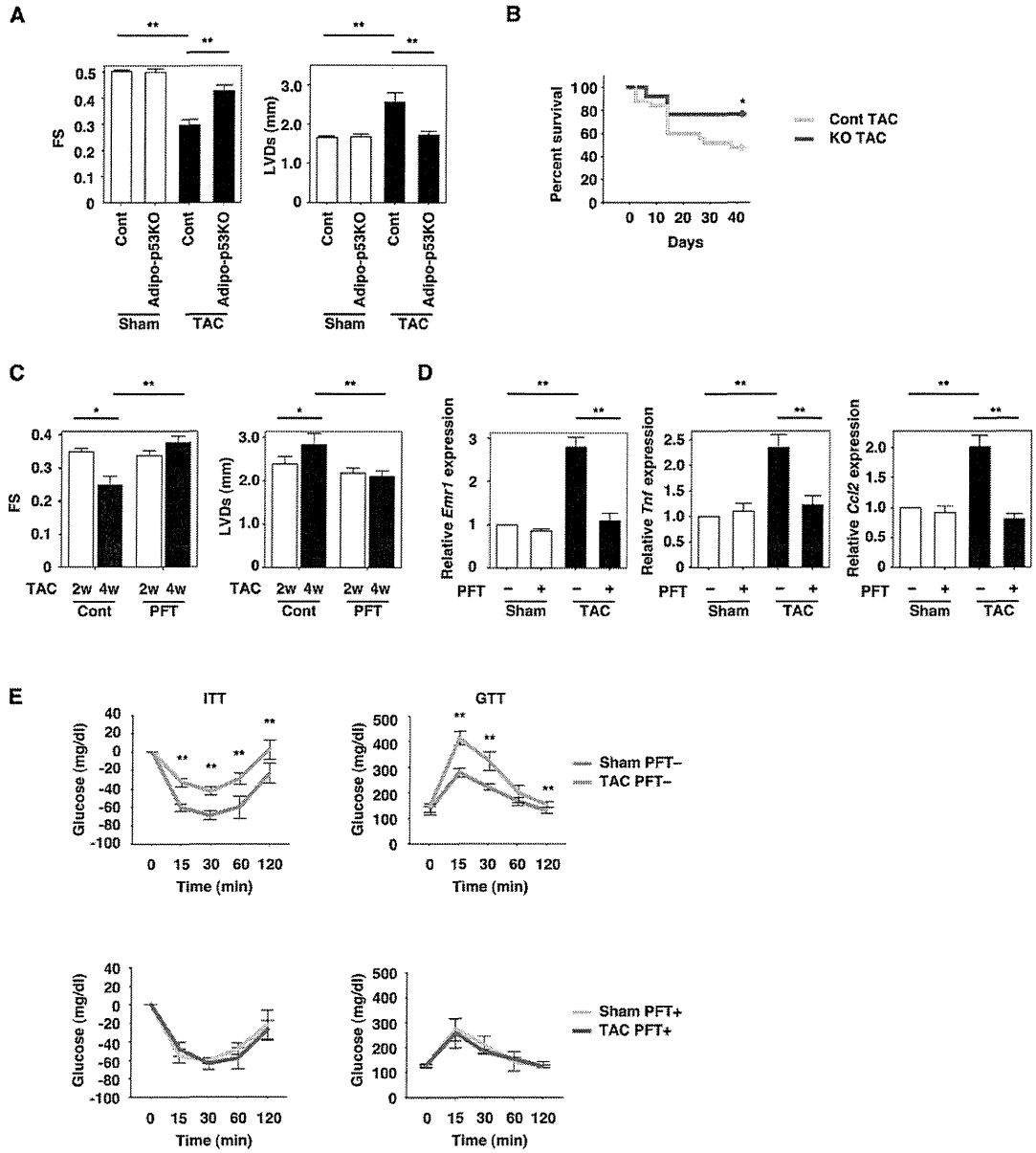

Figure 6. Influence of Inhibiting p53-Induced Adipose Tissue Inflammation on Cardiac Function

(A) Echocardiography to assess systolic function (FS) and ventricular size (LVDs) in adipocyte-specific p53-deficient mice (adipo-p53 KO) and littermate controls (Cont) at 6 weeks after sham operation or TAC (n = 8). FS, fractional shortening; LVDs, left ventricular end-systolic diameter.

(B) Survival rate of adipocyte-specific p53-deficient mice (adipo-p53 KO) and littermate controls (Cont) after TAC procedure (n = 25).

(C) Pifithrin-α (PFT) was administered into the adipose tissue of mice at 2–4 weeks after TAC, and systolic function (FS) and ventricular size (LVDs) were estimated before (2w, 2 weeks after TAC) and after (4w, 4 weeks after TAC) treatment by echocardiography (n = 5).

(D) Real-time PCR assessing the expression of *Emr1*, *Tnf* (Tnfα), and *Ccl2* (MCP1) levels in adipose tissue of mice at 4 weeks after sham operation or TAC with or without pifithrin-α (PFT) treatment (n = 4).

(E) Insulin tolerance test (ITT) and glucose tolerance test (GTT) of mice at 4 weeks after sham operation or TAC with or without pifithrin-α (PFT) treatment (n = 12).

Data are shown as the means ± S.E.M. *p < 0.05, **p < 0.01.

(Figures 7D and 7E), whereas knockdown of the NF-κB component p50 markedly inhibited palmitic acid-induced upregulation of *Ccl2* (Figure 7E). In addition, treatment with an antioxidant inhibited palmitic acid-induced DNA damage and upregulation of p53 (Figures S7A and S7B). We also found that ROS and γH2AX expression were increased in the adipose tissue of mice with heart failure (Figures 7F and 7G). Furthermore, nuclear localization of p50 was enhanced in adipose tissue during heart failure (Figures 7H and S7C). This increase of nuclear p50 expression and the upregulation of proinflammatory cytokines

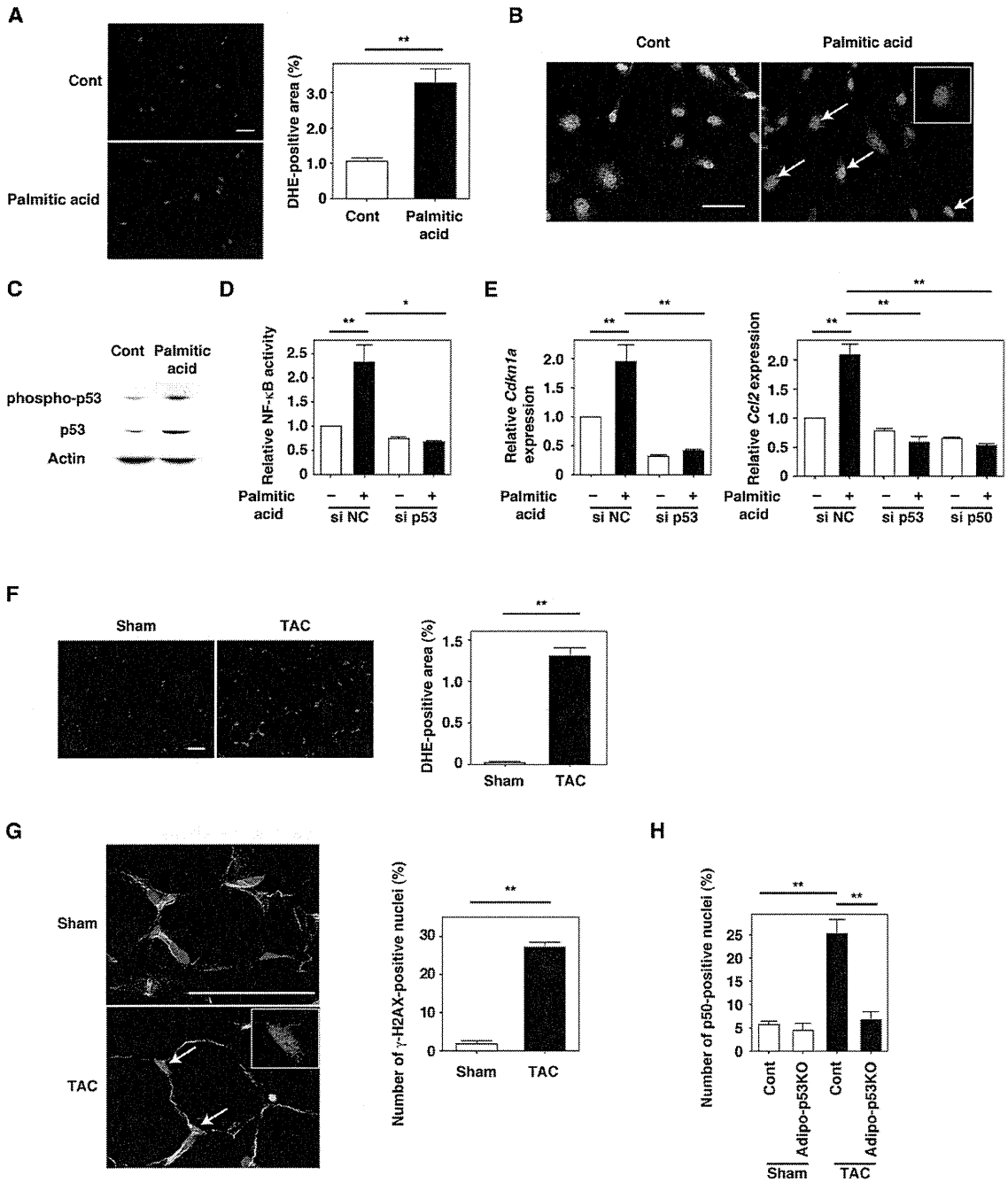

Figure 7. Mechanism of p53-Induced Adipose Tissue Inflammation during Heart Failure

(A) Dihydroethidium (DHE) staining (red) of preadipocytes treated with vehicle (Cont) or palmitic acid (500 μM) for 10 min. Nuclei were stained with Hoechst dye (blue). Scale bar indicates 50 μm. The right graph indicates the quantitative data on DHE-positive area (n = 4).

(B) Immunofluorescent staining for γ-H2AX (red) in preadipocytes treated with vehicle (Cont) or palmitic acid (500 μM) for 1 hr. Nuclei and plasma membranes were stained with Hoechst dye (blue) and Wheat Germ agglutinin lectin (green). Scale bar indicates 50 μm.

(C) Western blot analysis of phospho-p53 and p53 expression in preadipocytes treated with vehicle (Cont) or palmitic acid (500 μM).

(D) Small-interfering RNA targeting p53 (sip53) or negative control RNA (siNC) was introduced into preadipocytes treated with or without palmitic acid (500 μM) for 12 hr. The NF-κB activity was examined by luciferase assay (n = 5).

(E) Real-time PCR assessing the expression of *Cdkn1a* (p21) and *Ccl2* (MCP1) levels in preadipocytes prepared in Figure 7D (n = 9). The effect of small-interfering RNA targeting the NF-κB component p50 (sip50) on the expression of *Ccl2* (MCP1) was also examined (n = 9).

(F) Dihydroethidium (DHE) staining (red) in adipose tissue from sham-operated (Sham) and TAC mice. Nuclei were stained with Hoechst dye (blue). Scale bar indicates 20 μm. The right graph indicates the quantitative data on DHE-positive area (n = 5).

were inhibited by disruption of p53 in adipose tissue (Figures 2B, 7H, and S7C). Moreover, treatment with a lipolysis inhibitor significantly inhibited the heart failure-induced increase of ROS and nuclear p50 expression (Figures S7D and S7E). Inhibition of NF-κB activation in adipose tissue by BAY 11-7082 also significantly attenuated adipose tissue inflammation and improved metabolic abnormalities and cardiac dysfunction in TAC mice (Figures S7F–S7H). These results indicate that adrenergic activation by heart failure induces lipolysis in adipose tissue, which increases DNA damage due to ROS and thus upregulates p53. Activation of p53 then induces adipose tissue inflammation and metabolic abnormalities by upregulating the expression of NF-κB-dependent proinflammatory cytokines.

DISCUSSION

Although treatments that achieve neurohumoral antagonism have successfully reduced the morbidity and mortality of heart failure, the death rate remains unacceptably high (Kannel, 2000). Various metabolic abnormalities are associated with heart failure, and recent data have suggested that heart failure itself promotes adverse changes of metabolism, such as systemic insulin resistance (Ashrafian et al., 2007; Witteles and Fowler, 2008). Thus, a detrimental vicious cycle may be postulated, in which heart failure induces insulin resistance that in turn accelerates cardiac dysfunction (Opie, 2004). However, studies on the molecular mechanisms of such metabolic abnormalities in heart failure are largely preliminary and the results have sometimes been conflicting. In the present study, we demonstrated a causal role for heart failure in the development of insulin resistance by using two mouse models of heart failure, and we elucidated the underlying mechanisms. We found that the hyperadrenergic state of heart failure initiated a vicious metabolic cycle by promoting lipolysis in adipose tissue that increased the release of free fatty acids and upregulated p53 expression and proinflammatory cytokine production in adipose tissue, which then promoted systemic insulin resistance. Cardiac insulin resistance is considered to contribute to the development of heart failure. Because excessive cardiac insulin signaling has been reported to exacerbate systolic dysfunction in both TAC and MI models (Shimizu et al., 2010), hyperinsulinemia associated with systemic insulin resistance may also have a pathological role in heart failure until insulin resistance becomes evident in the myocardium. Inhibition of lipolysis by sympathetic denervation or by treatment with a lipolysis inhibitor improved insulin resistance in our heart failure model. Plasma free fatty acid levels were significantly elevated after the onset of heart failure, whereas this increase was attenuated by inhibition of lipolysis with acipimox, denervation, or guanethidine. Disruption of p53 in adipose tissue also markedly attenuated adipose inflammation and metabolic abnormalities associated with heart failure, whereas fatty acid levels were unaffected. Thus, adipose tissue inflammation rather than the increase of plasma free fatty acids per se is involved in the impairment of insulin sensitivity and glucose tolerance associated with heart failure. We also noted that p53 was modestly upregulated in the liver and skeletal muscle, presumably due to the increase of circulating free fatty acids. However, we did not detect a strong inflammatory response in those tissues under our experimental conditions (I. Shimizu and T. Minamino, unpublished data), suggesting that upregulation of adipose tissue p53 is more important for the development of metabolic abnormalities during heart failure. This concept is further supported by our finding that disruption of p53 activation in adipose tissue nearly normalized insulin resistance and glucose intolerance provoked by heart failure.

We observed that systolic cardiac function and survival with chronic heart failure were significantly better for adipo-p53 KO mice than their control littermates. Suppression of p53 activity in adipose tissue by administration of a p53 inhibitor after the onset of heart failure improved cardiac dysfunction and also reduced adipose tissue inflammation and metabolic abnormalities in both the TAC and MI models. Inhibition of NF-κB activity in adipose tissue also improved cardiac dysfunction, as well as adipose tissue inflammation and insulin resistance. Improvement of cardiac dysfunction by disruption of p53 in adipose tissue was not associated with a decrease of plasma free fatty acid levels. Systemic inhibition of lipolysis (Atgl deficiency or acipimox treatment) and disturbance of lipolysis in adipose tissue (denervation or guanethidine treatment) significantly reduced plasma free fatty acid levels (Haemmerle et al., 2006). However, the former intervention accelerated heart failure, whereas cardiac dysfunction was improved by the latter. Thus, the beneficial effect of inhibiting p53-induced adipose tissue inflammation on cardiac function is independent of changes in circulating free fatty acid levels, and lipolysis in cardiomyocytes appears to have a crucial role in cardiac metabolism and energy production. Although there is evidence suggesting that p53 has a protective role against damage due to ROS and lipotoxicity (Bazuine et al., 2009), our results indicate that chronic activation of p53 in adipose tissue causes inflammation and that inhibition of p53-induced adipose tissue inflammation is a potential target for treating metabolic abnormalities and systolic dysfunction in patients with heart failure.

Adipose tissue was traditionally considered to be a simple energy storage organ, but it is now appreciated that it also has endocrine functions and secretes a variety of factors referred to as adipokines (Donath and Shoelson, 2011; Hotamisligil, 2006; Ouchi et al., 2011). With high calorie intake, the size and number of adipocytes increase, and hypertrophic adipocytes shift the balance toward production of proinflammatory adipokines. This shift in the adipokine profile causes the modification of adipose tissue macrophages from the anti-inflammatory M2 type to the proinflammatory M1 type, and further increases the production of proinflammatory molecules, which in turn

(G) The number of γ-H2AX-positive nuclei (white arrows and inset) in adipose tissue of mice at 6 weeks after sham operation (Sham) or TAC procedure was estimated by immunofluorescent staining for γ-H2AX (red) (n = 5). Nuclei and plasma membranes were stained with Hoechst dye (blue) and Wheat Germ agglutinin lectin (green). Scale bar indicates 50 μm.

(H) The number of p50-positive nuclei in adipose tissue of adipocyte-specific p53-deficient mice (adipo-p53 KO) and littermate controls (Cont) at 6 weeks after sham operation (Sham) or TAC procedure was estimated by immunofluorescent staining for p50 (n = 6). Data are shown as the means ± S.E.M. *$p < 0.05$, **$p < 0.01$.

accelerates the recruitment of activated macrophages into inflamed fatty tissue. Adipokines produced by inflamed adipose tissue have been suggested to play a crucial role in the regulation of glucose and lipid metabolism and to contribute to the development of diabetes (Donath and Shoelson, 2011; Hotamisligil, 2006; Ouchi et al., 2011). It has been reported that excessive calorie intake leads to accumulation of ROS in adipose tissue and subsequently causes DNA damage that activates p53 (Minamino et al., 2009). In contrast to obesity, heart failure decreases body fat tissue mass by inducing lipolysis. Accelerated lipolysis and a subsequent increase of free fatty acids are likely to cause p53 activation because we found that the promotion of lipolysis by treatment with isoproterenol upregulated adipose tissue expression of p53, whereas inhibition of lipolysis by acipimox or disruption of lipase activity attenuated p53 expression. These results are consistent with a recent report describing that fasting-induced lipolysis promotes an immune response in murine adipose tissue (Kosteli et al., 2010). Various molecular mechanisms of p53 activation by heart failure may be postulated, including hypoxia, increased oxidative stress, and induction of endoplasmic reticulum stress (Harris and Levine, 2005; Schenk et al., 2008). Our in vitro and in vivo studies have indicated that an increase of free fatty acids causes ROS-induced DNA damage that upregulates p53 in adipose tissue. Activation of p53 then upregulates the expression of proinflammatory adipokines via the NF-κB signaling pathway and promotes systemic insulin resistance.

The β-blockers are competitive antagonists of β-adrenergic receptors. At one time, β-blockers were contraindicated in patients with heart failure due to their negative inotropic effect. However, several large-scale clinical trials demonstrated the efficacy of β-blockers for reducing morbidity and mortality in heart failure patients with impaired systolic function, so β-blockers are now recommended as first-line agent for these patients (Hjalmarson et al., 2000; Leizorovicz et al., 2002; Packer et al., 2001, 2002). A reduction of heart rate due to inhibition of cardiac β_1-adrenergic receptors is believed to be responsible for most of the therapeutic benefits associated with β-blocker treatment, although this is not the only mechanism of action that may be important in heart failure. It is interesting that treatment with a nonselective β-blocker (carvedilol) achieved a more marked improvement of survival in patients with chronic heart failure than treatment with a β_1-selective blocker (metoprolol) (Poole-Wilson et al., 2003), whereas new-onset diabetes was frequent in heart failure patients during treatment with the β_1-selective blocker (Torp-Pedersen et al., 2007). It has been reported that carvedilol antagonizes the β_3-adrenergic receptor as well as the $\beta_{1/2}$-adrenergic receptors (Schnabel et al., 2000). Taking our results together with these reports, it seems that inhibition of β_3-adrenergic activity in adipose tissue partially accounts for the better clinical outcome in patients treated with this nonselective β-blocker. Recent evidence has suggested that treatment with insulin sensitizers improves systolic function of the failing heart in animal models (Asakawa et al., 2002; Nemoto et al., 2005) but such treatment increases the incidence of heart failure in diabetic patients, presumably because of sodium retention (Home et al., 2009). Inhibition of p53-induced adipose tissue inflammation could be an alternative therapeutic target to block the metabolic vicious cycle in patients with heart failure.

EXPERIMENTAL PROCEDURES

Animal Models

All animal study protocols were approved by the Chiba University review board. C57BL/6 mice were purchased from the SLC Japan (Shizuoka, Japan). TAC and MI were performed in 11-week-old male mice as described previously (Harada et al., 2005; Sano et al., 2007). Sham-operated mice underwent the same procedure except for aortic constriction. Mice that expressed Cre recombinase in adipocytes (Fabp4-Cre) were purchased from Jackson Laboratories. We then crossed Fabp4-Cre mice (with a C57BL/6 background) with mice that carried floxed *Trp53* alleles with a C57BL/6 background (Marino et al., 2000) to generate adipocyte-specific p53 knockout mice. The genotype of littermate controls was Fabp4-Cre$^-$ *Trp53* $^{flox/flox}$. The generation and genotyping of Atgl-deficient mice has been described previously (Haemmerle et al., 2006). Surgical or chemical denervation was performed before TAC operation as described previously (Demas and Bartness, 2001; Foster and Bartness, 2006), with slight modification. In brief, the epididymal fat pad was gently separated from the skin and the abdominal wall by using a dissecting microscope. For surgical denervation, a drop of 1% toluidine blue was applied to the fat pad to facilitate visualization of the nerves. The nerves were then freed from the surrounding tissue and vasculature and cut in two or more locations, and the segments were removed to prevent possible reconnection. Chemical denervation was performed by the local injection of guanethidine sulfate (400 μg, Santa Cruz) into bilateral epididymal fat. Sham-operated mice for surgical denervation underwent the same procedure except for transection of the nerve. For the control group for chemical denervation, saline was injected into adipose tissue rather than guanethidine. Acipimox (Sigma) were provided in drinking water (at a concentration of 0.05%) for 6 weeks after TAC operation as described previously (Guo et al., 2009). Isoproterenol (30 mg/kg/day, Sigma) were delivered by infusion pump (DURECT Corporation) for 2 weeks as described previously (Iaccarino et al., 1999). The local injection of pifithrin-α (2.2 mg/kg/week, Carbiochem) or BAY 11-7082 (20 mg/kg/week, Carbiochem) into bilateral epididymal fat was performed to inhibit adipose p53 or NF-κB activity, respectively, from 2 weeks to 4 weeks after operation.

Physiological and Histological Analyses

Echocardiography was performed with a Vevo 770 High Resolution Imaging System (Visual Sonics Inc, Toronto, Ontario, Canada). To minimize variation of the data, the heart rate was always approximately 550–650 beats per minute when cardiac function was assessed. Epididymal fat samples were harvested and fixed in 10% formalin overnight. The samples were embedded in paraffin and sectioned (Narabyouri research Co., Ltd). The sections were subjected to immunohistochemistry or HE staining. The antibodies used are Mac3-specific primary antibody (PharMingen) for macrophages, p50-specific primary antibody (Cell signaling), and phospho-H2AX-specific antibody (Cell signaling).

Laboratory Tests

For the intraperitoneal glucose tolerance test (IGTT), mice were starved for 6 hr and were given glucose intraperitoneally at a dose of 2 g / kg (body weight) in the early afternoon. For the insulin tolerance test, mice were given human insulin intraperitoneally (1 U / kg body weight) at 1:00 pm without starvation. Blood glucose levels were measured with a glucose analyzer (Roche Diagnostics). We analyzed free fatty acid (Biovision, Inc) and norepinephrine levels (LDN) by using ELISA-based immunoassay kits according to the manufacturer's instruction.

Western Blot Analysis

The lysates were resolved by SDS-polyacrylamide gel electrophoresis. Proteins were transferred to a polyvinylidene difluoride membrane (Millipore, Bedford, MA), which was incubated with the primary antibody followed by anti-rabbit or anti-mouse immunoglobulin-G conjugated with horseradish peroxidase (Jackson, West Grove, PA).

Cell Culture

Human preadipocytes were purchased from Sanko (Tokyo, Japan) and were cultured according to the manufacturer's instructions. NIH 3T3-L1 cells were cultured in high-glucose DMEM plus 10% fetal bovine serum.

Ex Vivo Culture

Epididymal fat was extracted from Atgl-deficient or littermate mice at 17 weeks of age. Freshly isolated fat pads (100–120 mg) were incubated in Dulbecco's modified Eagle's medium supplemented with 10% fetal bovine serum in the presence of isoproterenol (10 μM) for 48 hr. Fat pads were treated with PBS instead of isoproterenol in the control group.

Statistical Analysis

Data are shown as the mean ± SEM. Differences between groups were examined by Student's t-test or ANOVA followed by Bonferroni's correction for comparison of means. For survival analysis, the Kaplan-Meier method and log-rank test were used. For all analyses, $p < 0.05$ was considered statistically significant.

SUPPLEMENTAL INFORMATION

Supplemental Information includes Supplemental Experimental Procedures and seven figures and can be found with this article online at doi:10.1016/j.cmet.2011.12.006.

ACKNOWLEDGMENTS

We thank A. Berns (The Netherlands Cancer Institute) for floxed p53 mice, T. Fujita (The Tokyo Metropolitan Institute of Medical Science) for reagents, and E .Takahashi, M. Iijima, and I. Sakamoto for their excellent technical assistance. This work was supported by a Grant-in-Aid for Scientific Research from the Ministry of Education, Culture, Sports, Science and Technology of Japan and grants from the Ono Medical Research Foundation; the Uehara Memorial Foundation; the Daiichi-Sankyo Foundation of Life Science; the NOVARTIS Foundation for the Promotion Science; the Japan Diabetes Foundation; the Mitsui Life Social Welfare Foundation; the Naito Foundation; the Japanese Society of Anti-Aging Medicine; and the Mitsubishi Pharma Research Foundation (to T.M.); a Grant-in-Aid for Scientific Research from the Ministry of Education, Science, Sports, and Culture and Health and Labor Sciences Research Grants (to I.K.); and a Grant-in-Aid for Scientific Research from the Ministry of Education, Science, Sports, and Culture, and Health and a grant from the Uehara Memorial Foundation, Takeda Science Foundation, and Kowa Life Science Foundation (to I.S.).

Received: June 10, 2011
Revised: October 27, 2011
Accepted: December 9, 2011
Published online: January 3, 2012

REFERENCES

Arnlöv, J., Lind, L., Zethelius, B., Andrén, B., Hales, C.N., Vessby, B., and Lithell, H. (2001). Several factors associated with the insulin resistance syndrome are predictors of left ventricular systolic dysfunction in a male population after 20 years of follow-up. Am. Heart J. *142*, 720–724.

Asakawa, M., Takano, H., Nagai, T., Uozumi, H., Hasegawa, H., Kubota, N., Saito, T., Masuda, Y., Kadowaki, T., and Komuro, I. (2002). Peroxisome proliferator-activated receptor gamma plays a critical role in inhibition of cardiac hypertrophy in vitro and in vivo. Circulation *105*, 1240–1246.

Ashrafian, H., Frenneaux, M.P., and Opie, L.H. (2007). Metabolic mechanisms in heart failure. Circulation *116*, 434–448.

Bazuine, M., Stenkula, K.G., Cam, M., Arroyo, M., and Cushman, S.W. (2009). Guardian of corpulence: a hypothesis on p53 signaling in the fat cell. Clin. Lipidol. *4*, 231–243.

Benoit, V., de Moraes, E., Dar, N.A., Taranchon, E., Bours, V., Hautefeuille, A., Tanière, P., Chariot, A., Scoazec, J.Y., de Moura Gallo, C.V., et al. (2006). Transcriptional activation of cyclooxygenase-2 by tumor suppressor p53 requires nuclear factor-kappaB. Oncogene *25*, 5708–5718.

Demas, G.E., and Bartness, T.J. (2001). Novel method for localized, functional sympathetic nervous system denervation of peripheral tissue using guanethidine. J. Neurosci. Methods *112*, 21–28.

Donath, M.Y., and Shoelson, S.E. (2011). Type 2 diabetes as an inflammatory disease. Nat. Rev. Immunol. *11*, 98–107.

Edwards, M.G., Anderson, R.M., Yuan, M., Kendziorski, C.M., Weindruch, R., and Prolla, T.A. (2007). Gene expression profiling of aging reveals activation of a p53-mediated transcriptional program. BMC Genomics *8*, 80.

Floras, J.S. (2009). Sympathetic nervous system activation in human heart failure: clinical implications of an updated model. J. Am. Coll. Cardiol. *54*, 375–385.

Foster, M.T., and Bartness, T.J. (2006). Sympathetic but not sensory denervation stimulates white adipocyte proliferation. Am. J. Physiol. Regul. Integr. Comp. Physiol. *291*, R1630–R1637.

Guo, W., Wong, S., Pudney, J., Jasuja, R., Hua, N., Jiang, L., Miller, A., Hruz, P.W., Hamilton, J.A., and Bhasin, S. (2009). Acipimox, an inhibitor of lipolysis, attenuates atherogenesis in LDLR-null mice treated with HIV protease inhibitor ritonavir. Arterioscler. Thromb. Vasc. Biol. *29*, 2028–2032.

Haemmerle, G., Lass, A., Zimmermann, R., Gorkiewicz, G., Meyer, C., Rozman, J., Heldmaier, G., Maier, R., Theussl, C., Eder, S., et al. (2006). Defective lipolysis and altered energy metabolism in mice lacking adipose triglyceride lipase. Science *312*, 734–737.

Harada, M., Qin, Y., Takano, H., Minamino, T., Zou, Y., Toko, H., Ohtsuka, M., Matsuura, K., Sano, M., Nishi, J., et al. (2005). G-CSF prevents cardiac remodeling after myocardial infarction by activating the Jak-Stat pathway in cardiomyocytes. Nat. Med. *11*, 305–311.

Harris, S.L., and Levine, A.J. (2005). The p53 pathway: positive and negative feedback loops. Oncogene *24*, 2899–2908.

Hjalmarson, A., Goldstein, S., Fagerberg, B., Wedel, H., Waagstein, F., Kjekshus, J., Wikstrand, J., El Allaf, D., Vítovec, J., Aldershvile, J., et al; MERIT-HF Study Group. (2000). Effects of controlled-release metoprolol on total mortality, hospitalizations, and well-being in patients with heart failure: the Metoprolol CR/XL Randomized Intervention Trial in congestive heart failure (MERIT-HF). JAMA *283*, 1295–1302.

Home, P.D., Pocock, S.J., Beck-Nielsen, H., Curtis, P.S., Gomis, R., Hanefeld, M., Jones, N.P., Komajda, M., and McMurray, J.J.; RECORD Study Team. (2009). Rosiglitazone evaluated for cardiovascular outcomes in oral agent combination therapy for type 2 diabetes (RECORD): a multicentre, randomised, open-label trial. Lancet *373*, 2125–2135.

Hotamisligil, G.S. (2006). Inflammation and metabolic disorders. Nature *444*, 860–867.

Hotamisligil, G.S., Shargill, N.S., and Spiegelman, B.M. (1993). Adipose expression of tumor necrosis factor-alpha: direct role in obesity-linked insulin resistance. Science *259*, 87–91.

Iaccarino, G., Dolber, P.C., Lefkowitz, R.J., and Koch, W.J. (1999). Bbeta-adrenergic receptor kinase-1 levels in catecholamine-induced myocardial hypertrophy: regulation by beta- but not alpha1-adrenergic stimulation. Hypertension *33*, 396–401.

Ingelsson, E., Sundström, J., Arnlöv, J., Zethelius, B., and Lind, L. (2005). Insulin resistance and risk of congestive heart failure. JAMA *294*, 334–341.

Kamei, N., Tobe, K., Suzuki, R., Ohsugi, M., Watanabe, T., Kubota, N., Ohtsuka-Kowatari, N., Kumagai, K., Sakamoto, K., Kobayashi, M., et al. (2006). Overexpression of monocyte chemoattractant protein-1 in adipose tissues causes macrophage recruitment and insulin resistance. J. Biol. Chem. *281*, 26602–26614.

Kannel, W.B. (2000). Incidence and epidemiology of heart failure. Heart Fail. Rev. *5*, 167–173.

Kosteli, A., Sugaru, E., Haemmerle, G., Martin, J.F., Lei, J., Zechner, R., and Ferrante, A.W., Jr. (2010). Weight loss and lipolysis promote a dynamic immune response in murine adipose tissue. J. Clin. Invest. *120*, 3466–3479.

Leizorovicz, A., Lechat, P., Cucherat, M., and Bugnard, F. (2002). Bisoprolol for the treatment of chronic heart failure: a meta-analysis on individual data of two placebo-controlled studies—CIBIS and CIBIS II. Cardiac Insufficiency Bisoprolol Study. Am. Heart J. *143*, 301–307.

Lopaschuk, G.D., Folmes, C.D., and Stanley, W.C. (2007). Cardiac energy metabolism in obesity. Circ. Res. *101*, 335–347.

Maier, B., Gluba, W., Bernier, B., Turner, T., Mohammad, K., Guise, T., Sutherland, A., Thorner, M., and Scrable, H. (2004). Modulation of mammalian life span by the short isoform of p53. Genes Dev. *18*, 306–319.

Marino, S., Vooijs, M., van Der Gulden, H., Jonkers, J., and Berns, A. (2000). Induction of medulloblastomas in p53-null mutant mice by somatic inactivation of Rb in the external granular layer cells of the cerebellum. Genes Dev. *14*, 994–1004.

Meek, D.W. (2009). Tumour suppression by p53: a role for the DNA damage response? Nat. Rev. Cancer *9*, 714–723.

Minamino, T., and Komuro, I. (2007). Vascular cell senescence: contribution to atherosclerosis. Circ. Res. *100*, 15–26.

Minamino, T., and Komuro, I. (2008). Vascular aging: insights from studies on cellular senescence, stem cell aging, and progeroid syndromes. Nat. Clin. Pract. Cardiovasc. Med. *5*, 637–648.

Minamino, T., Orimo, M., Shimizu, I., Kunieda, T., Yokoyama, M., Ito, T., Nojima, A., Nabetani, A., Oike, Y., Matsubara, H., et al. (2009). A crucial role for adipose tissue p53 in the regulation of insulin resistance. Nat. Med. *15*, 1082–1087.

Nemoto, S., Razeghi, P., Ishiyama, M., De Freitas, G., Taegtmeyer, H., and Carabello, B.A. (2005). PPAR-gamma agonist rosiglitazone ameliorates ventricular dysfunction in experimental chronic mitral regurgitation. Am. J. Physiol. Heart Circ. Physiol. *288*, H77–H82.

Neubauer, S. (2007). The failing heart—an engine out of fuel. N. Engl. J. Med. *356*, 1140–1151.

Nikolaidis, L.A., Sturzu, A., Stolarski, C., Elahi, D., Shen, Y.T., and Shannon, R.P. (2004). The development of myocardial insulin resistance in conscious dogs with advanced dilated cardiomyopathy. Cardiovasc. Res. *61*, 297–306.

Opie, L.H. (2004). The metabolic vicious cycle in heart failure. Lancet *364*, 1733–1734.

Ouchi, N., Parker, J.L., Lugus, J.J., and Walsh, K. (2011). Adipokines in inflammation and metabolic disease. Nat. Rev. Immunol. *11*, 85–97.

Packer, M., Coats, A.J., Fowler, M.B., Katus, H.A., Krum, H., Mohacsi, P., Rouleau, J.L., Tendera, M., Castaigne, A., Roecker, E.B., et al; Carvedilol Prospective Randomized Cumulative Survival Study Group. (2001). Effect of carvedilol on survival in severe chronic heart failure. N. Engl. J. Med. *344*, 1651–1658.

Packer, M., Fowler, M.B., Roecker, E.B., Coats, A.J., Katus, H.A., Krum, H., Mohacsi, P., Rouleau, J.L., Tendera, M., Staiger, C., et al; Carvedilol Prospective Randomized Cumulative Survival (COPERNICUS) Study Group. (2002). Effect of carvedilol on the morbidity of patients with severe chronic heart failure: results of the carvedilol prospective randomized cumulative survival (COPERNICUS) study. Circulation *106*, 2194–2199.

Poole-Wilson, P.A., Swedberg, K., Cleland, J.G., Di Lenarda, A., Hanrath, P., Komajda, M., Lubsen, J., Lutiger, B., Metra, M., Remme, W.J., et al; Carvedilol Or Metoprolol European Trial Investigators. (2003). Comparison of carvedilol and metoprolol on clinical outcomes in patients with chronic heart failure in the Carvedilol Or Metoprolol European Trial (COMET): randomised controlled trial. Lancet *362*, 7–13.

Royds, J.A., and Iacopetta, B. (2006). p53 and disease: when the guardian angel fails. Cell Death Differ. *13*, 1017–1026.

Ryan, K.M., Ernst, M.K., Rice, N.R., and Vousden, K.H. (2000). Role of NF-kappaB in p53-mediated programmed cell death. Nature *404*, 892–897.

Sano, M., Minamino, T., Toko, H., Miyauchi, H., Orimo, M., Qin, Y., Akazawa, H., Tateno, K., Kayama, Y., Harada, M., et al. (2007). p53-induced inhibition of Hif-1 causes cardiac dysfunction during pressure overload. Nature *446*, 444–448.

Schenk, S., Saberi, M., and Olefsky, J.M. (2008). Insulin sensitivity: modulation by nutrients and inflammation. J. Clin. Invest. *118*, 2992–3002.

Schnabel, P., Maack, C., Mies, F., Tyroller, S., Scheer, A., and Böhm, M. (2000). Binding properties of beta-blockers at recombinant beta1-, beta2-, and beta3-adrenoceptors. J. Cardiovasc. Pharmacol. *36*, 466–471.

Sharma, N., Okere, I.C., Duda, M.K., Chess, D.J., O'Shea, K.M., and Stanley, W.C. (2007). Potential impact of carbohydrate and fat intake on pathological left ventricular hypertrophy. Cardiovasc. Res. *73*, 257–268.

Shimizu, I., Minamino, T., Toko, H., Okada, S., Ikeda, H., Yasuda, N., Tateno, K., Moriya, J., Yokoyama, M., Nojima, A., et al. (2010). Excessive cardiac insulin signaling exacerbates systolic dysfunction induced by pressure overload in rodents. J. Clin. Invest. *120*, 1506–1514.

Suskin, N., McKelvie, R.S., Burns, R.J., Latini, R., Pericak, D., Probstfield, J., Rouleau, J.L., Sigouin, C., Solymoss, C.B., Tsuyuki, R., et al. (2000). Glucose and insulin abnormalities relate to functional capacity in patients with congestive heart failure. Eur. Heart J. *21*, 1368–1375.

Tenenbaum, A., Motro, M., Fisman, E.Z., Leor, J., Freimark, D., Boyko, V., Mandelzweig, L., Adler, Y., Sherer, Y., and Behar, S. (2003). Functional class in patients with heart failure is associated with the development of diabetes. Am. J. Med. *114*, 271–275.

Torp-Pedersen, C., Metra, M., Charlesworth, A., Spark, P., Lukas, M.A., Poole-Wilson, P.A., Swedberg, K., Cleland, J.G., Di Lenarda, A., Remme, W.J., and Scherhag, A.; COMET investigators. (2007). Effects of metoprolol and carvedilol on pre-existing and new onset diabetes in patients with chronic heart failure: data from the Carvedilol Or Metoprolol European Trial (COMET). Heart *93*, 968–973.

Tuunanen, H., Engblom, E., Naum, A., Någren, K., Hesse, B., Airaksinen, K.E., Nuutila, P., Iozzo, P., Ukkonen, H., Opie, L.H., and Knuuti, J. (2006). Free fatty acid depletion acutely decreases cardiac work and efficiency in cardiomyopathic heart failure. Circulation *114*, 2130–2137.

Tyner, S.D., Venkatachalam, S., Choi, J., Jones, S., Ghebranious, N., Igelmann, H., Lu, X., Soron, G., Cooper, B., Brayton, C., et al. (2002). p53 mutant mice that display early ageing-associated phenotypes. Nature *415*, 45–53.

Vousden, K.H., and Lane, D.P. (2007). p53 in health and disease. Nat. Rev. Mol. Cell Biol. *8*, 275–283.

Vousden, K.H., and Prives, C. (2009). Blinded by the Light: The Growing Complexity of p53. Cell *137*, 413–431.

Vousden, K.H., and Ryan, K.M. (2009). p53 and metabolism. Nat. Rev. Cancer *9*, 691–700.

Weisberg, S.P., McCann, D., Desai, M., Rosenbaum, M., Leibel, R.L., and Ferrante, A.W., Jr. (2003). Obesity is associated with macrophage accumulation in adipose tissue. J. Clin. Invest. *112*, 1796–1808.

Witteles, R.M., and Fowler, M.B. (2008). Insulin-resistant cardiomyopathy clinical evidence, mechanisms, and treatment options. J. Am. Coll. Cardiol. *51*, 93–102.

Young, M.E., McNulty, P., and Taegtmeyer, H. (2002). Adaptation and maladaptation of the heart in diabetes: Part II: potential mechanisms. Circulation *105*, 1861–1870.

Zeng, L., Wu, G.Z., Goh, K.J., Lee, Y.M., Ng, C.C., You, A.B., Wang, J., Jia, D., Hao, A., Yu, Q., and Li, B. (2008). Saturated fatty acids modulate cell response to DNA damage: implication for their role in tumorigenesis. PLoS ONE *3*, e2329.

Original Article

Patients with CD36 Deficiency Are Associated with Enhanced Atherosclerotic Cardiovascular Diseases

Miyako Yuasa-Kawase[1], Daisaku Masuda[1], Taiji Yamashita[1], Ryota Kawase[1], Hajime Nakaoka[1], Miwako Inagaki[1], Kazuhiro Nakatani[1], Kazumi Tsubakio-Yamamoto[1], Tohru Ohama[1,3], Akifumi Matsuyama[2], Makoto Nishida[1,3], Masato Ishigami[4], Toshiharu Kawamoto[5], Issei Komuro[1] and Shizuya Yamashita[1]

[1]Department of Cardiovascular Medicine, Osaka University Graduate School of Medicine, Osaka, Japan
[2]Department of Somatic Stem Cell Therapy, Institute of Biomedical Research and Innovation, Foundation for Biomedical Research and Innovation, TRI305, Hyogo, Japan
[3]Health Care Center, Osaka University, Osaka, Japan
[4]Department of Biomedical Informatics, Division of Health Sciences, Osaka University Graduate School of Medicine, Osaka, Japan
[5]Kure Heart Center, National Hospital Organization Kure Medical Center, Hiroshima, Japan

Aim: The clustering of dyslipidemia, impaired glucose tolerance and hypertension increases the morbidity and mortality from cardiovascular events. A class B scavenger receptor, CD36, is a receptor for oxidized LDL and a transporter of long-chain fatty acids. Because of the impaired uptake of oxidized LDL in CD36-deficient macrophages and from the results of CD36 knockout mice, CD36 deficiency (CD36-D) was supposed to be associated with reduced risks for coronary artery disease (CAD); however, CD36-D patients are often accompanied by a clustering of coronary risk factors. The current study aimed to investigate the morbidity and severity of cardiovascular diseases in CD36-D patients.
Methods: By screening for CD36 antigen on platelets and monocytes using FACS or the absent myocardial accumulation of ^{123}I-BMIPP by scintigraphy, 40 patients with type I CD36-D were collected, the morbidity of CAD and their features of atherosclerotic cardiovascular diseases were observed. Screening for CD36-D in both CAD patients (n=319) and healthy subjects (n=1,239) were underwent.
Results: The morbidity of CAD was significantly higher in CD36-D patients than in the general population; 50% of patients (20 out of 40) had CAD identified by BMIPP scintigraphy and 37.5% (3 out of 8) by FACS screening, respectively. Three representative CD36-D cases demonstrated severe CAD and atherosclerosis. The frequency of CD36-D was three times higher in CAD patients than in healthy subjects (0.9% vs 0.3%, $p<0.0001$).
Conclusion: The morbidity of CAD is significantly higher in CD36-D patients suffering from severe atherosclerosis, implying that the status of CD36-D might be atherogenic.

J Atheroscler Thromb, 2012; 19:263-275.

Key words; CD36 deficiency, Long-chain fatty acid transporter, Atherosclerotic cardiovascular disease, Insulin resistance, Metabolic syndrome

Introduction

Patients with metabolic syndrome (MetS) are characterized by a clustering of coronary risk factors, such as dyslipidemia including hypertriglyceridemia and a low level of high density lipoprotein-cholesterol (HDL-C), impaired glucose tolerance and hypertension along with the accumulation of abdominal visceral fat. The morbidity and mortality of atherosclerotic cardiovascular events are significantly high in patients with MetS, and the reduction of abdominal visceral fat by diet and exercise therapy is very important for treatment of the clustering of these coronary risk fac-

Address for correspondence: Shizuya Yamashita, MD, PhD, FAHA, FJCC, Department of Cardiovascular Medicine, Osaka University Graduate School of Medicine, 2-2 Yamadaoka, Suita, Osaka 565-0871, Japan
E-mail: shizu@imed2.med.osaka-u.ac.jp
Received: June 13, 2011
Accepted for publication: September 6, 2011

tors and atherosclerotic cardiovascular diseases.

CD36 is an 88-kDa membrane glycoprotein belonging to a class B scavenger receptor[1]. CD36 is expressed in a variety of cells and tissues including platelets, monocyte/macrophages, heart, skeletal muscle, adipose tissue and small intestines[1]. CD36 is a receptor for oxidized low density lipoproteins (LDL)[2] and a transporter of long-chain fatty acids (LCFA)[3]. CD36-deficient patients were first identified from subjects who were refractory to platelet transfusion[4]. Kashiwagi *et al.* identified several genetic mutations of human CD36 deficiency (CD36-D)[5]. We previously investigated the metabolic phenotypes of CD36-D patients[6-7] and reported that they (high fasting serum triglycerides level, low HDL-C level, fasting hyperglycemia, insulin resistance and hypertension) were frequently observed and clustered in patients with CD36-D, similar to those with MetS[8-9]. It was later reported that the accumulation of these metabolic phenotypes is not due to the deposition of abdominal visceral fat, but to insulin resistance or impaired metabolism of lipoproteins and free fatty acids (FFA) in the postprandial state in patients with CD36-D[8-10]. It is well known that these metabolic profiles are independent coronary risk factors in the general population[11-13]; therefore, the status of human CD36-D was supposed to be atherogenic and the morbidity of atherosclerotic cardiovascular diseases might be high in patients with CD36-D.

In contrast, the status of human CD36-D was supposed to be anti-atherogenic since CD36 is a scavenger receptor for oxidized LDL when the foam cell formation of CD36-D macrophages by exposure of oxidized LDL is impaired[14]. Nozaki et al. showed that the uptake of oxidized LDL was reduced by approximately 40% in macrophages from patients with CD36-D compared with normal controls[15]. Janabi *et al.* showed that the responses of oxidized LDL-induced NF-kappa B activation and subsequent cytokine expression were impaired in monocyte-derived macrophages from CD36-D patients[16]. Furthermore, there have been two reports by Febbraio *et al.* and Moore *et al.* concerning the atherogenicity of genetic disruption of CD36 in mice[17-18]. Both reports showed that macrophage foam cell formation when treated with oxidized LDL was impaired when they crossed CD36 null mice with atherogenic apoE-null mice; however, atherosclerotic lesion development in CD36-apoE double knockout mice was different in these two reports. Febbraio *et al.* showed a 76.5% decrease in aortic tree lesion areas when mice were fed a Western diet and a 45% decrease in the aortic sinus lesion area when fed a normal diet in CD36-apoE double knockout mice, respectively, compared with wild-type mice[17]. In contrast, Moore et al. showed that CD36-apoE double knockout (DKO) mice did not show amelioration of the progression of atherosclerotic lesions but foam cell accumulation at aortic sinus rather increased and the severity of atherosclerotic lesions was advanced in DKO mice compared with apoE-KO mice[18]. From these controversial results, the atherogenicity of CD36-D, especially that of human CD36-D patients, remains unclear.

We have so far identified 40 patients with CD36-D by myocardial scintigraphy using an analogue of LCFA, ^{123}I-BMIPP, or by screening with immunofluorescent flow cytometric analysis (FACS). We experienced three typical cases of severe atherosclerotic cardiovascular diseases in patients with CD36-D who were identified in our previous study[9] and evaluated by imaging studies. In the current study, in order to elucidate whether the morbidity and severity of atherosclerotic cardiovascular diseases are high in patients with CD36-D, we evaluated the prevalence of atherosclerotic cardiovascular diseases in 40 patients with CD36-D. Furthermore, to exclude the patient collection bias and to extend the knowledge to the general population, we compared the prevalence of CD36-D between patients with CAD and healthy subjects. We demonstrate that the morbidity of CAD is significantly higher in CD36-D patients suffering from severe atherosclerosis, implying that the status of human CD36-D might be atherogenic.

Subjects and Methods

Diagnosis of CD36 Deficiency

In our previous study, 40 patients without myocardial accumulation of an LCFA analogue, ^{123}I-beta-methyl-p-iodophenyl-pentadecanoic acid (^{123}I-BMIPP), were identified among patients whose heart was evaluated by single photon emission computed tomography (SPECT) for the evaluation of cardiac performance screening at Osaka University Hospital and related hospitals[9]. In order to confirm the diagnosis of CD36-D in these patients, immunofluorescent flow cytometric analysis was performed by using mouse monoclonal antibodies against CD36 (OKM5; Ortho Diagnostic System Inc., Raritan, NJ) at the Department of Blood Transfusion, Osaka University Hospital[7]. Briefly, 20 ml of blood was drawn, anticoagulated with heparin (10 U/ml), layered over 10 ml Ficoll-Paque (GE Healthcare UK Ltd., Buckinghamshire, UK) and centrifuged at 1,000 g for 30 minutes. A 50 μl suspension of platelets ($2\times10^5/\mu$l) or mononuclear cells ($2\times10^4/\mu$l) was incubated with FITC-conjugat-

ed anti-human CD36 monoclonal antibody OKM5 (Ortho Diagnostic Systems) (final concentration: 2.5 μg/ml) or FITC-conjugated mouse IgG (final concentration: 2.5 μg/ml) for 30 minutes at 40℃ and assayed on a FACScan® system (Becton Dickinson Co., Mountain View, CA) as previously reported[7]. Appropriate cell fractions for the analysis of monocytes were selected by a gating method with a two-dimensional display of forward scatter and side scatter of analyzed cells[15]. We diagnosed patients with type I CD36-D whose CD36 antigen was not detected in either monocytes or platelets. Each subject gave written informed consent before participating in the study, and the ethics committee of Osaka University Hospital approved the study design.

Analysis of Clinical Profile and Atherosclerotic Cardiovascular Diseases in Patients with CD36-D

The presence or absence of atherosclerotic cardiovascular diseases was extensively investigated in patients with CD36-D based upon their medical history and symptoms. We assessed the severity of atherosclerotic cardiovascular diseases and risk factors of these patients. Blood pressure was determined in the sitting position, and peripheral venous blood was drawn in the fasting state after overnight fasting and centrifuged for serum separation. Serum levels of total cholesterol (TC), triglycerides (TG), and HDL-cholesterol (HDL-C) as well as fasting plasma glucose levels were measured by enzymatic methods as reported in our previous study[9]. HbA1c was measured by HPLC (Sekisui Medical Co., Tokyo, Japan). All samples were treated in accordance with the Helsinki Declaration. In some patients with CD36-D, coronary angiography was performed for an extensive evaluation of coronary artery atherosclerosis. In order to evaluate atherosclerotic lesions in arteries other than coronary arteries in detail, the thoracic and abdominal aorta and their branches were examined by aortic angiography or magnetic resonance angiography.

Prevalence of CAD in Patients with CD36-D Identified by Absence of Cardiac Uptake of ^{123}I-BMIPP

In order to assess whether patients with CD36-D had a higher mortality and severity of CAD, we evaluated the morbidity of CAD in these patients by checking medical records. The diagnosis of CAD was established when a patient had coronary artery stenosis (≥ 75%) assessed by coronary angiography. The CAD patients were divided into 3 groups by their clinical course and results of coronary angiography: 1) acute or old myocardial infarction, 2) unstable angina, and 3) stable angina.

Prevalence of CAD in Patients with CD36-D Identified by Screening of CD36-D by FACS Analysis in the General Population

For the screening study of CD36-D by FACS analysis, normal healthy volunteers were recruited for over ten years in our laboratory and we found 8 patients with type I CD36-D. We traced their medical records, especially the result of coronary angiography, in order to confirm whether they were accompanied by CAD.

Prevalence of CD36-D in Patients with CAD and Healthy Subjects

In order to evaluate whether the frequency of CD36-D in patients with CAD is higher than in normal healthy subjects, we performed screening examinations in patients with CAD and healthy subjects. Patients with coronary artery stenoses (≥ 75%) were diagnosed with CAD by coronary angiography (n=319). Normal healthy volunteers were recruited using the following criteria: no ST-T abnormalities in ECG, no chest symptoms on effort and no significant coronary artery stenosis (≥ 75%) if they received coronary angiography (n=1,239). Their cell surface CD36 antigen on monocytes and platelets was analyzed by FACS analysis and type I CD36-D was diagnosed by an absence of CD36 antigen in both cells. Statistical significance was assessed by Pearson's chi-square test using JMP 8 software (SAS Institute Japan, Tokyo, Japan).

Results

Case Presentations

Out of 40 patients with CD36-D, we experienced three representative cases of severe atherosclerotic cardiovascular diseases. The metabolic parameters of these patients are shown in **Table 1**, and compared with those of patients with CD36-D in our previous study[9]. As found in that study, these three cases were accompanied by hypertriglyceridemia and low HDL-C, and hypertension (Case 2 received anti-hypertensive drugs), while one case showed high fasting plasma glucose.

Case 1 is a 74-year-old man. At the age of 62, he suffered acute myocardial infarction. Coronary angiography demonstrated severe and diffuse stenoses in 3 major coronary arteries (**Fig. 1A** and **1B**) and he underwent percutaneous coronary revascularization. At the age of 66, angiographic restenosis was detected in the right coronary artery (RCA) and left anterior descending artery (LAD), which were later revascularized successfully. At the same time, we found total oc-

Table 1. Metabolic Profiles of Three Cases of CD36-D Associated with Severe Atherosclerotic Cardiovascular Diseases

	Case 1	Case 2	Case 3	CD36-D ($n=40$)*	Healthy subjects ($n=84$)*
Age (year)	74	73	73	62 ± 14	60 ± 14
Sex (m/f)	male	male	female	(25, 15)	(63, 21)
BMI (kg/m^2)	21.6	24	21.4	23.5 ± 3.6	23.5 ± 2.0
TC (mg/dl)	193	166	220	201 ± 39	205 ± 32
TG (mg/dl)	192	152	156	178 ± 89	126 ± 62
HDL-C (mg/dl)	29	34	34	46 ± 15	61 ± 11
FPG (mg/dl)	100	87	210	110 ± 22	95 ± 18
sBP (mmHg)	152	128	154	135 ± 18	115 ± 15
dBP (mmHg)	94	86	53	80 ± 10	77 ± 18

*CD36-D ($n=40$) and healthy, age, sex, and BMI-matched controls ($n=84$) were quoted from our previous study (Reference 9).
Abbreviations: BMI, body mass index; TC, total cholesterol; TG, triglycerides; FPG, fasting plasma glucose; sBP, systolic blood pressure; dBP, diastolic blood pressure.

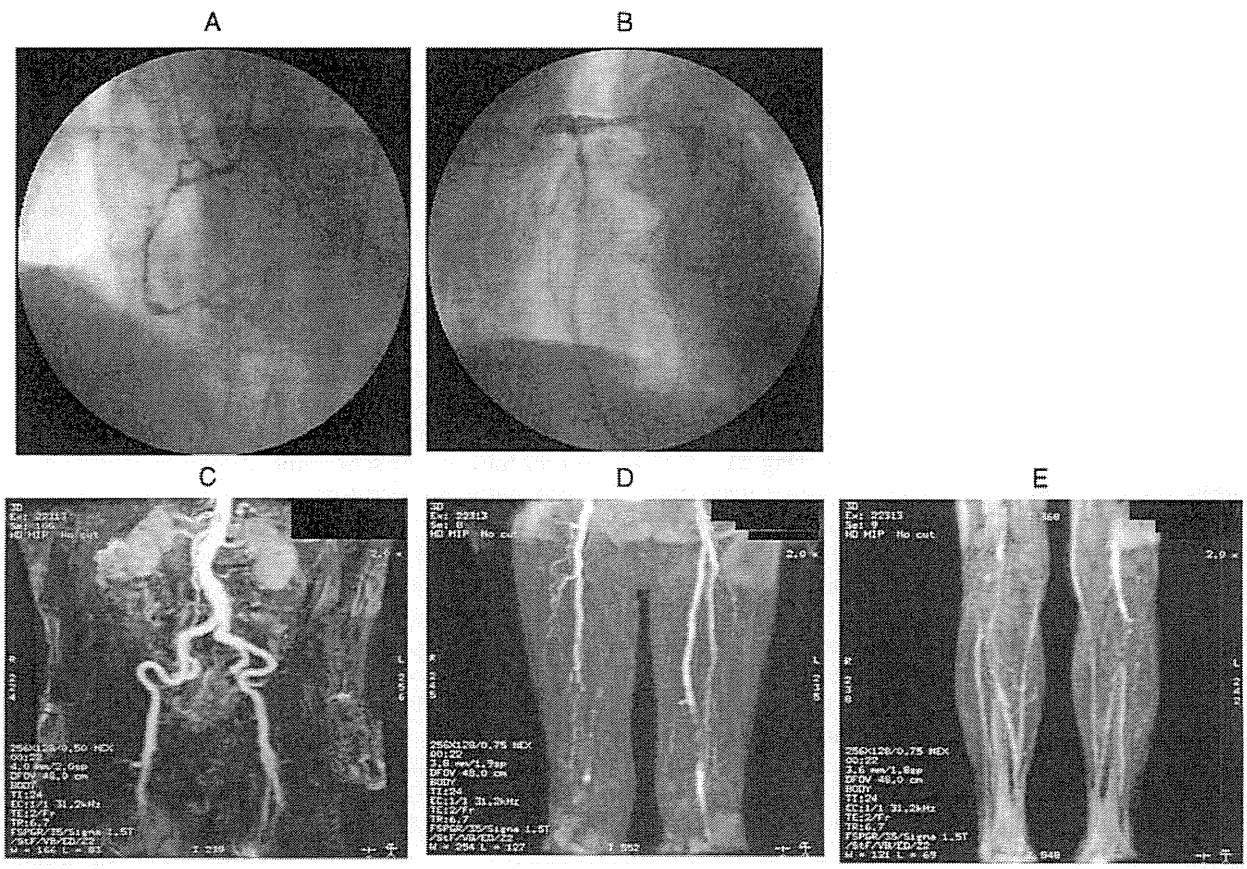

Fig. 1. Case 1, a 74-year-old male patient with CD36-D

At the age of 62, he suffered from acute myocardial infarction, and emergent cardiac catheterization revealed severe and diffuse stenosis in the triple coronary arteries (1-A, right coronary artery (RCA); 1-B, left coronary artery (LCA), respectively). Magnetic resonance angiography revealed total occlusion of bilateral femoral arteries (1-C and 1-D), total occlusion of left anterior tibial artery and severe stenosis of right anterior tibial artery (1-E).

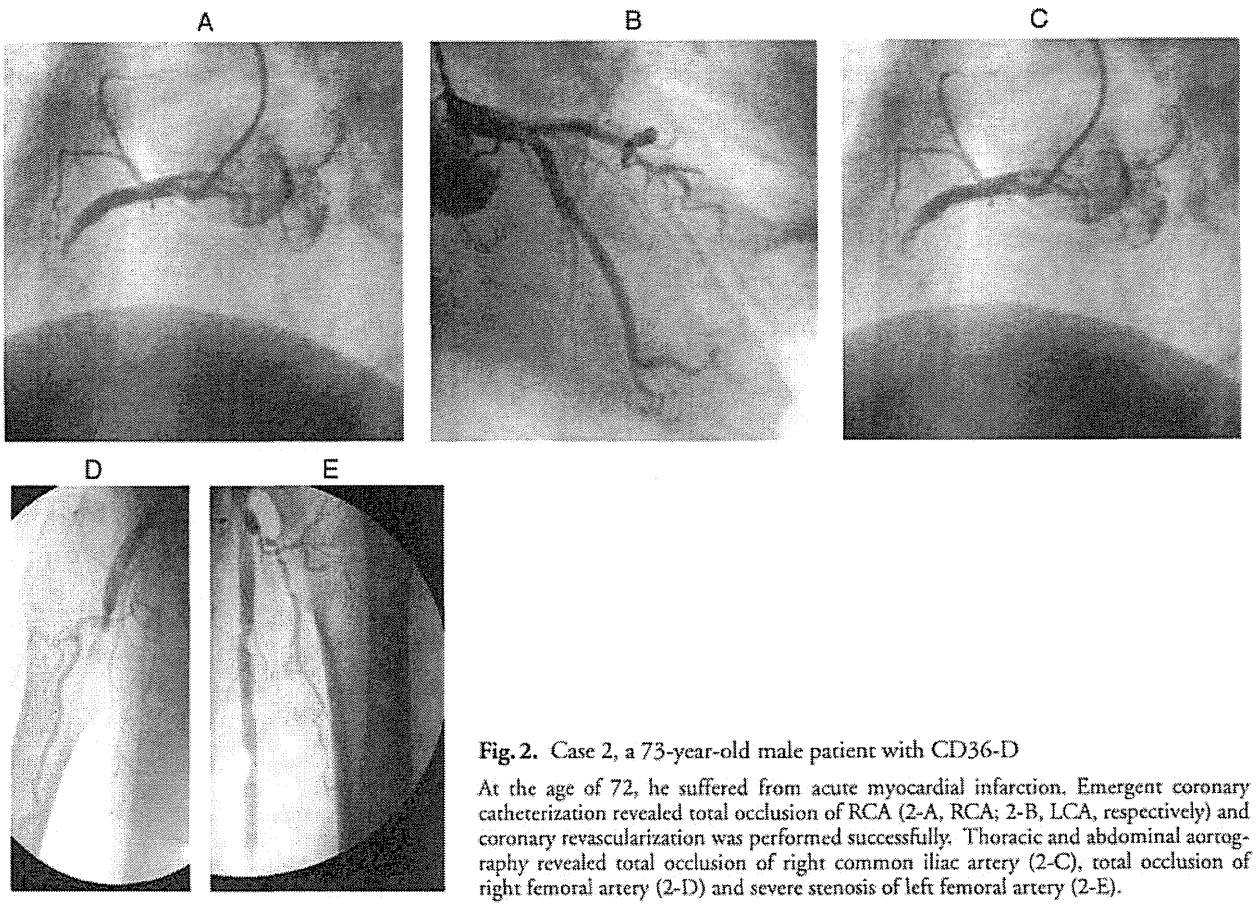

Fig. 2. Case 2, a 73-year-old male patient with CD36-D

At the age of 72, he suffered from acute myocardial infarction. Emergent coronary catheterization revealed total occlusion of RCA (2-A, RCA; 2-B, LCA, respectively) and coronary revascularization was performed successfully. Thoracic and abdominal aortography revealed total occlusion of right common iliac artery (2-C), total occlusion of right femoral artery (2-D) and severe stenosis of left femoral artery (2-E).

clusion of bilateral femoral arteries (**Fig. 1C** and **1D**), complete obstruction of the left anterior tibial artery and severe stenosis of the right anterior tibial artery by magnetic resonance angiography (MRA) (**Fig. 1E**). Up to the age of 73, the serum level of brain natriuretic peptide (BNP) gradually increased and left ventricular ejection fraction assessed by echocardiography gradually decreased, although repeated revascularization was undergone successfully. At the age of 74, ^{123}I-BMIPP scintigraphy revealed no myocardial uptake of BMIPP, an analogue of LCFA, and he was diagnosed with type I CD36-D by FACS analysis. Regarding his risk factors for cardiovascular diseases, he had a history of smoking and impaired glucose tolerance was observed by an oral glucose tolerance test (data not shown) in addition to the metabolic disorders shown in **Table 1**.

Case 2 is a 73 year-old man. He had a history of excessive alcohol consumption, but he had never smoked. For over 10 years he regularly attended Osaka University Hospital and received medical treatments for hypertension and intermittent claudication. At the age of 72, he suffered acute myocardial infarction. On emergent coronary angiography, total occlusion of RCA was identified (**Fig. 2A** and **2B**), and thereafter coronary revascularization was performed successfully. At the same time, thoracic and abdominal aortography revealed total occlusion of the right common iliac artery (**Fig. 2C**), complete obstruction of the right femoral artery (**Fig. 2D**) and severe stenosis of the left femoral artery (**Fig. 2E**). Thus, we decided to start anticoagulant therapy. Left ventricular ejection fraction in echocardiography did not improve although coronary revascularization was successful; therefore, we tested whether LCFA metabolism was impaired by scintigraphy using ^{123}I-BMIPP, an analogue of LCFA, and found marked reduction of myocardial uptake of ^{123}I-BMIPP. He was finally diagnosed with type I CD36-D by FACS analysis. This was accompanied by moderate hypertension and dyslipidemia, including hypertriglyceridemia and low HDL-C, as shown in **Table 1**.

Case 3 is a 73 year-old woman. She had no history of smoking or regular alcohol intake. At the age of 64, she began to feel chest discomfort and muscle

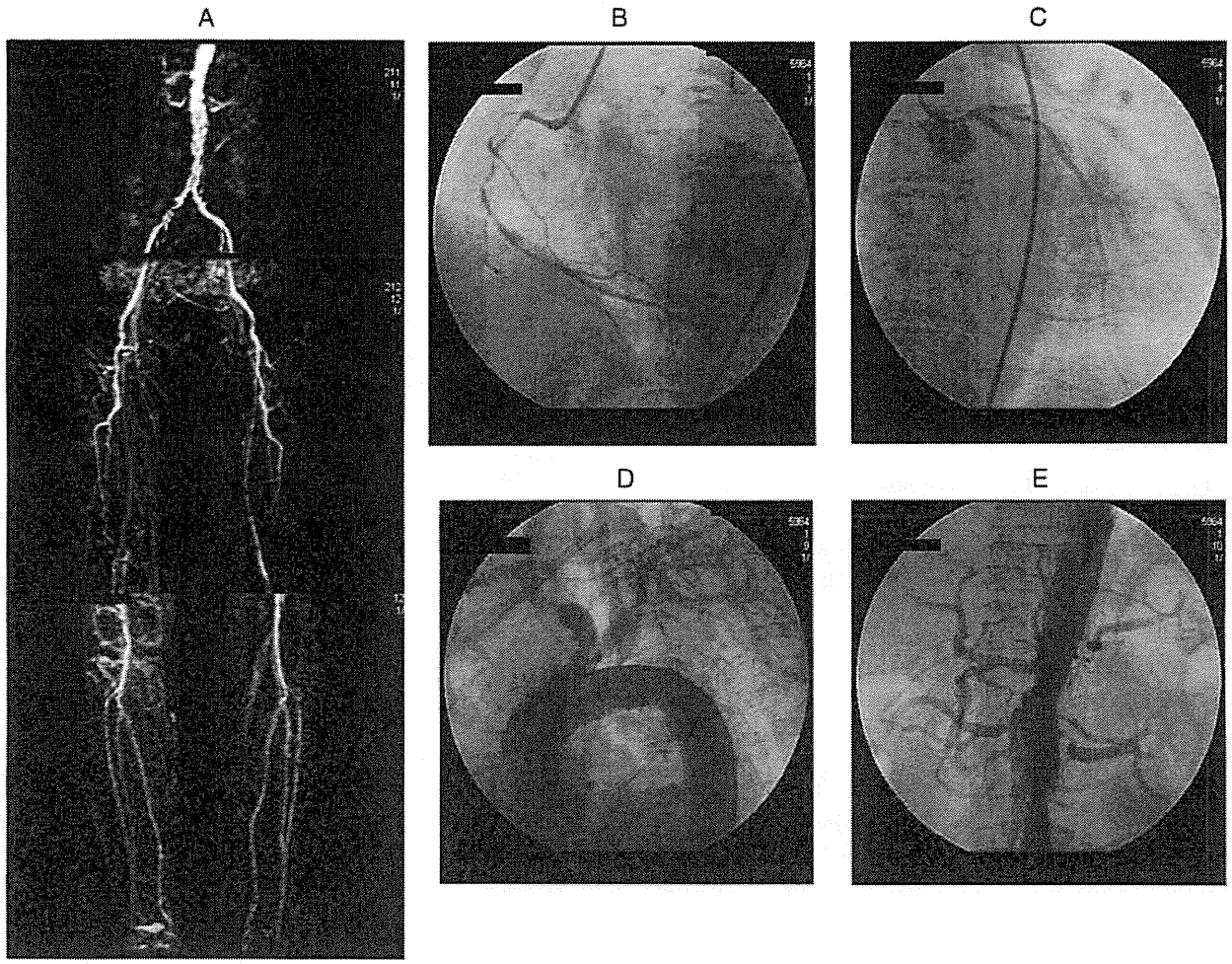

Fig. 3. Case 3, a 73-year-old female patient with CD36-D

At the age of 64, she felt chest discomfort and muscle fatigue of the bilateral legs after climbing stairs. Magnetic resonance angiography (MRA) of lower limbs revealed total occlusion of bilateral femoral arteries and severe stenosis of right common iliac artery and bilateral popliteal arteries (3-A). The following year she was hospitalized for refractory unstable angina, and diagnostic cardiac catheterization revealed severe stenosis of triple coronary arteries (3-B and 3-C). Thoracic and abdominal aortography revealed severe stenosis of trunks brachiocephalicus, right common carotid artery (3-D), abdominal aorta and left renal artery (3-E).

fatigue of the bilateral legs after climbing stairs. MRA of the lower limbs revealed total occlusion of the bilateral femoral arteries and severe stenosis of the right common iliac artery and bilateral popliteal arteries (**Fig. 3A**); therefore, anticoagulant drugs and vasodilators were administered. The following year she was hospitalized because of refractory unstable angina. Emergent diagnostic cardiac catheterization and thoracic and abdominal aortography were performed, which revealed severe stenoses of triple coronary arteries (**Fig. 3B** and **3C**), the brachiocephalic trunk, right common carotid artery (**Fig. 3D**), abdominal aorta and left renal artery (**Fig. 3E**). At the same time, the patient was diagnosed with type II diabetes, hypertension, hypertriglyceridemia and low HDL-C, and drug treatments were started for these diseases. After stent implantation in the left renal artery, coronary artery bypass graft surgery was performed and a saphenous vein graft was connected to the RCA and left circumflex coronary artery, and the left internal thoracic artery to LAD. At the age of 73, she began to complain of exertional dyspnea and the serum level of BNP gradually increased even though these grafts were patent and native coronary arteries remained intact, as assessed by coronary angiography. ^{123}I-BMIPP scintigraphy revealed no myocardial uptake of BMIPP and she

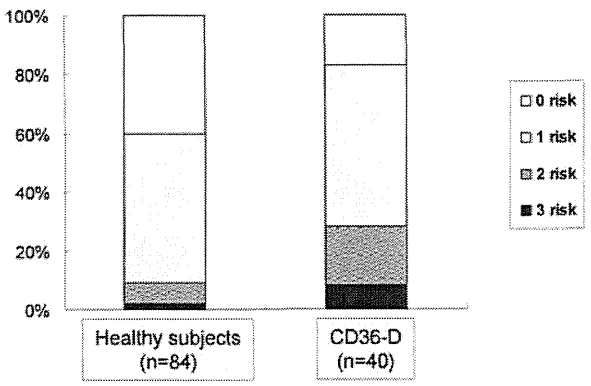

Fig. 4. Number of risk factors for CAD in patients with CD36-D

Patients with CD36-D (n=40) and healthy, age-, sex-, and BMI-matched controls (n=84) were from our previous study (Reference 9). Diabetes mellitus, hypertension and dyslipidemia were counted as risk factors for CAD. Patients with CD36-D had more risk factors for CAD than healthy subjects (patients with CD36-D vs healthy subjects: 1.20±0.80 vs 0.76±0.72 risk factors, P=0.005), and were associated with multiple risk factors for CAD.

was diagnosed with type I CD36-D by FACS analysis.

Number of Risk Factors for CAD in Patients with CD36-D and Healthy Control Subjects

We compared the number of risk factors for CAD in patients with CD36-D (n=40) and healthy, age, sex, and BMI-matched control subjects (n=84) from our former study[9]. These risk factors included diabetes mellitus, hypertension and dyslipidemia. As shown in **Fig. 4**, patients with CD36-D had more risk factors for CAD than healthy subjects (1.20±0.80 vs. 0.76±0.72 risks, p=0.005), and were often associated with multiple risk factors for CAD.

Frequency of CAD in Patients with CD36-D

The frequency of CAD was examined among 40 patients with CD36-D who were identified by an absence of cardiac uptake of ^{123}I-BMIPP. As shown in **Table 2**, the frequency of CAD in CD36-D patients was significantly high (50%, 20 of 40 CD36-D patients). Furthermore, in 20 CD36-D cases of CAD, coronary stenoses with high severity, acute or old myocardial infarction and unstable angina pectoris were observed in 65% (13 of 20 patients with CD36-D). These data suggest that CD36-D patients are accompanied by enhanced atherosclerotic cardiovascular diseases. By a screening study of FACS analysis, we found 8 patients with type I CD36 deficiency. Three patients (37.5%) out of 8 had coronary artery stenoses by coronary angiography.

Table 2. Frequency of Coronary Artery Disease in Patients with CD36 Deficiency

Patients with CD36-D (n=40)	
BMIPP	
CAD negative	50% (20/40)
CAD positive	50% (20/40)
acute MI	22.5% (9/40)
unstable angina	10% (4/40)
stable angina	17.5% (7/40)
Screening Study by FACS	
CAD negative	62.5% (5/8)
CAD positive	37.5% (3/8)

Abbreviations: BMIPP, ^{123}I-beta-methyl-p-iodophenyl-pentadecanoic acid; CAD, coronary artery disease; CD36-D, CD36 deficiency; MI, myocardial infarction.

Table 3. Frequency of CD36-D in Patients with Coronary Artery Disease

	Patients with CAD (n=319)	Healthy subjects (n=1239)
Frequency of CD36-D	0.94%* (3/319)	0.32% (4/1239)

*p<0.0001, assessed by Pearson's chi-square test

Prevalence of CD36-D in Patients with CAD and Healthy Subjects

In order to investigate whether CD36-D may increase the prevalence of CAD, we also compared the morbidity of CD36-D between healthy subjects (n=1,239) and patients with CAD diagnosed by coronary angiography (n=319). As shown in **Table 3**, the frequency of CD36-D in patients with CAD was approximately 3-fold higher than in healthy subjects [CAD patients vs healthy subjects, 0.94 % (3/319) vs 0.32 % (4/1239)]. The statistical significance was assessed by Pearson's chi-square test, and the frequency of CD36-D was significantly higher in patients with CAD (p<0.0001). These data suggest that patients with CD36-D are susceptible to CAD.

Discussion

In patients with CD36-D, compared with healthy CD36-positive controls, metabolic phenotypes such as high TG levels, low HDL-C levels, high fasting glucose and hypertension were observed more frequent-

ly[7, 9]. Furthermore, we also found that patients with CD36-D are accompanied by insulin resistance[10], postprandial hyperlipidemia, and high levels of remnant lipoprotein cholesterol and FFA[8-9]. These coronary risk factors were clustered in each CD36-D patient, which may appear to be partly similar to the profiles of patients with MetS[8-9]. Another report showed that Pro90Ser CD36 mutation was associated with elevated FFA levels[19]. These profiles have been shown to be independent coronary risk factors by many clinical investigations[11-13]; however, the morbidity of atherosclerotic cardiovascular diseases in patients with CD36-D has not been clarified beside the reports of Ma *et al.*[20] and Yasunaga *et al.*[21]. Ma *et al*[20] showed that a common haplotype at the CD36 locus was associated with high FFA levels and increased cardiovascular risk in Caucasians. Yasunaga *et al.*[21] reported a 45-year-old male CD36-D patient with acute coronary syndrome without major cardiovascular risk factors. Emergency coronary angiography demonstrated 90% stenosis at segment 7 of LAD. We compared the number of risk factors for CAD in patients with CD36-D and healthy subjects (**Fig. 4**). Patients with CD36-D had more risk factors for CAD than healthy subjects and were associated with multiple risk factors for CAD. We also suggested that the clustering of coronary risk factors might increase the morbidity of cardiovascular disease in patients with CD36-D compared with healthy subjects.

In the current study, we investigated for the first time whether the morbidity of atherosclerotic cardiovascular diseases in CD36-D patients is higher. The clinical observations of three representative CD36-D patients were demonstrated in detail for those whose atherosclerotic lesions of not only coronary arteries but also the aorta and its branches could be assessed. As demonstrated in **Table 1**, dyslipidemia, hypertension and hyperglycemia were clustered in these three cases. Aortography and MRA revealed severe and multiple stenoses and occlusion of the aorta, its branches and arteries of lower limbs. We also found that atherosclerotic lesions were relatively long (up to 8-10 cm) and their collateral circulation was developed sufficiently. It was suggested that multiple and sequential stenoses along with long distance occlusion were not due to acute thrombotic occlusion but to chronic progression of atherosclerotic plaques. These three patients were rather older than the average CD36-D patients and were associated with multiple risk factors; therefore, we could not exclude the possibility that aging and the simple clustering of risk factors might have enhanced the atherogenicity in these three cases; however, a similar tendency of the clustering of CAD risk factors and the association of atherosclerotic cardiovascular diseases were also observed in younger patients with CD36-D.

We also investigated the morbidity and severity of atherosclerotic cardiovascular diseases in 40 patients with CD36-D who were identified by BMIPP scintigraphy and a screening study by FACS analysis. As shown in **Table 2**, we found extremely high morbidity of CAD (50%, 20 of 40 patients with CD36-D). Among 20 CD36-D patients with CAD, 13 (65%) were accompanied by unstable angina or acute myocardial infarction due to the stenosis and occlusion of coronary arteries; therefore, these data suggest that the morbidity and severity of CAD were significantly higher in patients with CD36-D than CD36-positive control subjects. Furthermore, many patients with both CD36-D and CAD suffered from other atherosclerotic cardiovascular diseases involving the stenosis and occlusion of arteries in the upper and lower limbs.

Since ^{123}I-BMIPP scintigraphy was performed in order to evaluate the myocardial damage of FFA metabolism in subjects with possible ischemic heart disease, the possibility could not be rejected that the 40 patients in the current study were extracted from a population with high morbidity of CAD. Watanabe *et al.*[22] also reported patients with type I and type II CD36-D, many of whom were accompanied by CAD or cardiomyopathy, although these patients were found by ^{123}I-BMIPP scintigraphy. Therefore, in the current study, we also examined the morbidity of CAD from a screening study. The morbidity of CAD was 50% in CD36-D patients identified by ^{123}I-BMIPP scintigraphy, while 37.5% (3 CAD of 8 CD36-D patients) in the population in the screening study. Although these data further imply that the morbidity of CAD in patients with CD36-D is definitely high, the possibility of patient selection bias cannot be excluded.

To explore further the contribution of CD36-D to the development of CAD in the general population, we compared by FACS analysis the frequency of CD36-D between patients with CAD diagnosed by coronary angiography (n=322) and non-CAD subjects (n=1,239). As shown in **Table 3**, the frequency of CD36-D was significantly three times higher in patients with CAD than in non-CAD subjects; therefore, the risk for the development of CAD is significantly higher in CD36-D patients, although the uptake of oxidized LDL *in vitro* is reduced in monocyte-derived macrophages.

Since foam cell formation by the uptake of oxidized LDL was shown to be reduced in monocyte-derived macrophages of CD36-D patients, it may be necessary to explore novel mechanisms for the en-

hanced atherogenicity in a CD36-deficient condition. We will discuss these mechanisms in more detail as follows (**Fig. 5**):

1) Increased Lipoprotein Remnants and Postprandial Hyperlipidemia

In the postprandial state of CD36-D patients, we demonstrated that not only hypertriglyceridemia but also increased levels of apoB-48, chylomicron remnants, and small dense LDL were observed[9]. In our previous papers, we demonstrated that CD36-null mice showed higher TG concentrations in plasma and intestinal lymph than wild-type mice even in a high fat loading state, suggesting that CD36-null mice may have intestinal overproduction of chylomicrons and may be a good mouse model of postprandial hyperlipidemia[23-24]. Furthermore, patients with CD36-D were also associated with insulin resistance, as we reported[10]. These profiles associated with impaired lipid and glucose metabolism proved to be independent coronary risk factors in the general CD36-positive population[11-13]. Moreover, these profiles were linked; the increase in chylomicron remnants in the postprandial state was shown to be associated with insulin resistance[25]; the production of small dense LDL was shown to be associated with the impaired postprandial clearance of TG-rich lipoproteins including remnants[26-27]; the accumulation of TG-rich lipoproteins caused an increase in FFA levels; high levels of FFA may suppress lipoprotein lipase (LPL) activity and the clearance of TG-rich lipoproteins, resulting in increased remnants[28]. Therefore, these lipoprotein phenotypes clustered in patients with CD36-D might have a synergistic influence and enhance the cardiovascular risk. Furthermore, as nicely reviewed by Fujioka *et al.*[29], increased remnant lipoproteins (mainly chylomicron remnants) contribute to form atherosclerotic lesions through a variety of mechanisms. It was demonstrated that chylomicron remnants invade directly into the subendothelial spaces of arteries and are taken up by macrophages via several receptors, such as LDL receptor-related protein (LRP) or apoB-48 receptor, resulting in macrophage foam cell formation[30-33]. We reported that increased serum chylomicron remnants are directly associated with enhanced carotid atherosclerosis in subjects with apparently normal TG levels[34]. Chylomicron remnants induce the secretion of monocyte chemoattractant protein 1 (MCP-1), which stimulates the migration of monocytes through arterial endothelial layers[35] and the production of plasminogen activator inhibitor-I (PAI-I), which regulates thrombus formation on endothelial cells[33]. Thus, abundant chylomicron remnants in the blood of CD36-D patients might enhance the foam cell formation of CD36-deficient macrophages, leading to the development of atherosclerotic cardiovascular diseases.

2) Reduced Serum HDL-C Levels

In CD36-D patients, we demonstrated a reduction of serum HDL-C[9], although there is a report showing an increase of serum HDL-C[36]. More recently, Love-Gregory *et al.*[37] reported a homozygote of SNP32 who was CD36-D accompanied by hypertriglyceridemia and reduction of serum HDL-C, although heterozygotes showed an opposite profile. The reduced serum HDL-C in our CD36-D patients could be one of the causes of enhanced atherogenicity.

3) Increased Free Fatty Acids Levels Caused by Deficiency of LCFA Transporter

CD36 is distributed in the heart, skeletal muscles and adipose tissues where it functions as one of the transporters of LCFA[38]. CD36 may be a major transporter of LCFA in the heart, since the uptake of ^{123}I-BMIPP, an analogue of LCFA, in cardiac scintigraphy is markedly deficient in CD36-D patients, which causes increased serum FFA and the 2-fold-enhanced influx of LCFA into the liver[39]. Increased FFA flux into the liver may cause overproduction of VLDL and hypertriglyceridemia as well as insulin resistance.

4) Insulin Resistance and Impaired Glucose Metabolism

CD36-D was shown to be accompanied by insulin resistance[10, 40-43]; however, this is controversial[36, 44]. CD36 knockout mice developed marked glucose intolerance, hyperinsulinemia and decreased muscle glucose uptake on a fructose-rich diet, but not on a high-starch, low-fat diet[42]. Goudriaan *et al.*[43] demonstrated that CD36-D increases insulin sensitivity in muscle, but induces insulin resistance in the liver. Insulin resistance may lead to the down-regulation of lipoprotein lipase and finally to hypertriglyceridemia.

5) Hypertension

The average systolic and diastolic blood pressure in our CD36-D patients was significantly high compared with CD36-positive subjects, similar to the reported case of MetS and vasospastic angina[45]. The mechanism for increased blood pressure is unknown; however, it may accelerate the development of atherosclerosis.

6) Increased PAI-I Levels

Low plasma fibrinolytic activity in association with increased PAI-I levels has been demonstrated to